

# Modeling and Interpreting Patient Subgroups in Hospital Readmission: Visual Analytical Approach

Suresh K. Bhavnani, Ph.D.,<sup>1,2§</sup> Weibin Zhang, Ph.D.,<sup>1</sup> Shyam Visweswaran, M.D., Ph.D.,<sup>3,4</sup>  
Mukaila Raji, M.D., M.S., F.A.C.P.,<sup>5</sup> Yong-Fang Kuo, Ph.D.<sup>1</sup>

<sup>1</sup>School of Public and Population Health, University of Texas Medical Branch, Galveston, TX, USA

<sup>2</sup>Institute for Translational Sciences, University of Texas Medical Branch, Galveston, TX, USA

<sup>3</sup>Department of Biomedical Informatics, University of Pittsburgh, Pittsburgh, PA, USA

<sup>4</sup>Intelligent Systems Program, University of Pittsburgh, Pittsburgh, PA, USA

<sup>5</sup>Division of Geriatric Medicine, Department of Internal Medicine, University of Texas Medical Branch Galveston, TX, USA

<sup>§</sup>Corresponding author

Suresh K. Bhavnani, Ph.D., M.Arch., FAMIA

School of Public and Population Health

Institute for Translational Sciences

University of Texas Medical Branch

301 University Blvd

Galveston, TX, USA

email: subhavna@utmb.edu

## ABSTRACT

### Background

A primary goal of precision medicine is to identify patient subgroups and infer their underlying disease processes, with the aim of designing targeted interventions. However, while several studies have identified patient subgroups, there is a considerable gap between the identification of patient subgroups, and their modeling and interpretation for clinical applications.

### Objectives

To develop and evaluate a novel analytical framework for modeling and interpreting patient subgroups (MIPS) using a three-step modeling approach. (1) *Visual analytical* modeling to automatically identify patient subgroups and their co-occurring comorbidities, and determine their statistical significance and clinical interpretability. (2) *Classification* modeling to classify patients into subgroups and measure its accuracy. (3) *Prediction* modeling to predict a patient's risk for an adverse outcome, and compare its accuracy with and without patient subgroup information.

### Methods

The MIPS framework was developed using (1) bipartite networks to identify patient subgroups based on frequently co-occurring high-risk comorbidities; (2) multinomial logistic regression to classify patients into subgroups; and (3) hierarchical logistic regression to predict the risk of an adverse outcome using subgroup membership, compared to standard logistic regression without subgroup membership. The MIPS framework was evaluated on three hospital readmission conditions: chronic obstructive pulmonary disease (COPD), congestive heart failure (CHF), and total hip/knee arthroplasty (THA/TKA). For each condition, we extracted cases defined as patients readmitted within 30 days of hospital discharge, and controls defined as patients not readmitted within 90 days of discharge, matched by age, gender, race, and Medicaid eligibility ( $n[\text{COPD}]=29,016$ ,  $n[\text{CHF}]=51,550$ ,  $n[\text{THA/TKA}]=16,498$ ).

### Results

In each condition, the visual analytical model identified patient subgroups that were statistically significant ( $Q=0.17, 0.17, 0.31$ ;  $P<.001, <.001, <.05$ ), were significantly replicated ( $RI=0.92, 0.94, 0.89$ ;  $P<.001, <.001, <.01$ ), and were clinically meaningful to clinicians. (2) In each condition, the classification model had high accuracy in classifying patients into subgroups (mean accuracy=99.60%, 99.34%, 99.86%). (3) In two conditions (COPD, THA/TKA), the hierarchical prediction model had a small but statistically significant improvement in discriminating between the readmitted and not readmitted patients as measured by net reclassification improvement ( $\text{NRI}=.059, .11$ ), but not as measured by the C-statistic or integrated discrimination improvement (IDI).

### Conclusions

While the visual analytical models identified statistically and clinically significant patient subgroups, the results pinpoint the need to analyze subgroups at different levels of granularity for improving the interpretability of intra- and inter-cluster associations. The high accuracy of the classification models reflects the strong separation of the patient subgroups despite the size and density of the datasets. Finally, the small improvement in predictive accuracy suggests that comorbidities alone were not strong predictors for hospital readmission, and the need for more sophisticated subgroup modeling methods. Such advances could improve the interpretability and predictive accuracy of patient subgroup models for reducing the risk of hospital readmission and beyond.

# INTRODUCTION

## Overview

A wide range of studies [1-9] on topics ranging from molecular to environmental determinants of health have shown that most humans tend to share a subset of characteristics (e.g., comorbidities, symptoms, genetic variants), forming distinct patient subgroups. A primary goal of precision medicine is to identify such patient subgroups and infer their underlying disease processes to design interventions targeted to those processes [2, 10]. For example, recent studies in complex diseases such as breast cancer [3, 4], asthma [5-7] and COVID-19 [11] have revealed patient subgroups, each with different underlying mechanisms precipitating the disease, and therefore each requiring different interventions.

However, there is a considerable gap between the identification of patient subgroups, and their modeling and interpretation for clinical applications. To bridge this gap, we developed and evaluated a novel analytical framework called Modeling and Interpreting Patient Subgroups (MIPS) using a three-step modeling approach: (1) identification of patient subgroups, their frequently co-occurring characteristics, and their risk for adverse outcomes, (2) classification of a new patient into one or more subgroups, and (3) prediction of an adverse outcome for a new patient informed by subgroup membership. We evaluated MIPS on three datasets related to hospital readmission, which helped to pinpoint the strengths and limitations of MIPS. The results provide implications of MIPS for improving the interpretability of patient subgroups in large and dense datasets, and for the design of clinical decision support systems to prevent adverse outcomes such as hospital readmissions.

## Identification of Patient Subgroups

Patients have been divided into subgroups by using (a) investigator-selected variables such as race for developing hierarchical regression models [12], or assigning patients to different arms of a clinical trial, (b) existing classification systems such as the Medicare Severity-Diagnosis Related Group (MS-DRG) [13] to assign patients into a disease category for purposes of billing, and (c) computational methods such as classification [14-16] and clustering [5, 17] to discover patient subgroups from data (also referred to as *subtypes* or *phenotypes* depending on the condition and variables analyzed).

Several studies have used computational methods to identify patient subgroups, each with critical trade-offs. Some studies have used *combinatorial* approaches [18] (identify all pairs, all triples etc.), which are intuitive, but which can lead to a combinatorial explosion (e.g., enumerating combinations of the 31 Elixhauser comorbidities would lead to  $2^{31}$  or 2147483648 combinations), with most combinations that do not incorporate the full range of symptoms (e.g., the most frequent pair of symptoms ignores what other symptoms exist in the profile of patients with that pair). Other studies have used *unipartite* clustering methods [16, 17] (clustering patients or comorbidities, but not both together) such as k-means, and hierarchical clustering; and dimensionality-reduction methods such as principal component analysis (PCA) to help identify clusters of frequently co-occurring comorbidities [18-24]. However, such methods have well-known limitations including the requirement of inputting user-selected parameters (e.g., similarity measures, and the number of expected clusters), in addition to the lack of a quantitative measure to describe the quality of the clustering (critical for measuring the statistical significance of the clustering). Furthermore, because these methods are unipartite, there is no agreed-upon method to identify the patient subgroup defined by a cluster of variables, and vice-versa.

More recently, bipartite network analysis [25] has been used to address the above limitations by automatically identifying *biclusters*, consisting of patients and characteristics simultaneously. This method takes as input any dataset such as patients and their comorbidities, and outputs a quantitative and visual description of biclusters (containing both patients subgroups and their frequently co-occurring comorbidities). The quantitative output generates the number, size, and statistical significance of the biclusters [26-28], and the visual output displays the quantitative information of the biclusters through a network visualization [29-31]. Bipartite network analysis therefore enables (1) the automatic identification of biclusters and their significance, and (2) the visualization of the biclusters critical for their clinical interpretability. Furthermore, the attributes of patients in a subgroup can be used to measure the subgroup risk for an adverse outcome, to develop classifiers for classifying a new patient into one or more of the subgroups, and to develop a predictive model that uses that subgroup membership for measuring the risk of an adverse outcome for the classified patient.

However, while several studies [11, 28, 32-38] have demonstrated the usefulness of bipartite networks for the identification and clinical interpretation of patient subgroups, there has been no systematic attempt to integrate them with classification and prediction modeling, a critical step towards clinical application. We therefore leveraged the advantages of bipartite network to develop the MIPS framework, with the goal of bridging the gap between the identification and interpretation of patient subgroups, and their future clinical application.

## The Need for Modeling and Interpreting Patient Subgroups in Hospital Readmission

An estimated one in five elderly patients (over 2.3 million Americans) is readmitted to a hospital within 30-days after being discharged [39]. While many readmissions are unavoidable, an estimated 75% of readmissions are unplanned and mostly preventable [40], imposing a significant burden in terms of mortality, morbidity, and resource consumption. Across all conditions, unplanned readmissions cost almost \$17 billion annually in the US [40], making them an ineffective use of costly resources, and therefore closely scrutinized as a marker for the poor quality of care by organizations such as the Centers for Medicare & Medicaid Services (CMS) [41].

To address this epidemic of hospital readmission, CMS sponsored the development of models to predict the patient-specific risk of readmission in specific index conditions such as chronic obstructive pulmonary disease (COPD) [42], congestive heart failure (CHF) [43], and hip/knee arthroplasty (THA/TKA) [44]. The independent variables include prior comorbidities (as recorded in Medicare claims data), and demographics (age, gender, and race). This was motivated by numerous studies that have shown that almost two-thirds of older adults have two or more comorbid conditions, which have a heightened risk for adverse health outcomes such as hospital readmission [45]. However, although prior studies have shown the existence of subgroups among patients with hospital readmission [28], none of the CMS models incorporated patient subgroups. The identification and inclusion of patient subgroups could improve the accuracy of predicting hospital readmission for a patient, in addition to enabling the design of interventions targeted to each patient subgroup for reducing the risk of readmission. We therefore used the MIPS framework to model and interpret patient subgroups in hospital readmission, and tested its generality across three index conditions. Furthermore, to enable a head-to-head comparison with the existing CMS predictive models, we used the same independent variables in addition to patient subgroup membership, when developing our prediction models.

## METHOD

### Overview of MIPS

Fig. 1 provides a conceptual description of the data inputs and outputs from the three-step modeling in MIPS. As shown, the visual analytical model identifies the patient subgroups, and visualizes them through a network. The classification model predicts subgroup membership for cases and controls, and uses it to measure the risk of readmission within each subgroup based on its proportion of cases. This risk information is juxtaposed with the visualization to enable clinicians interpret the readmitted patient subgroups. Finally, the predictive model

### Modeling and Interpreting Patient Subgroups (MIPS)

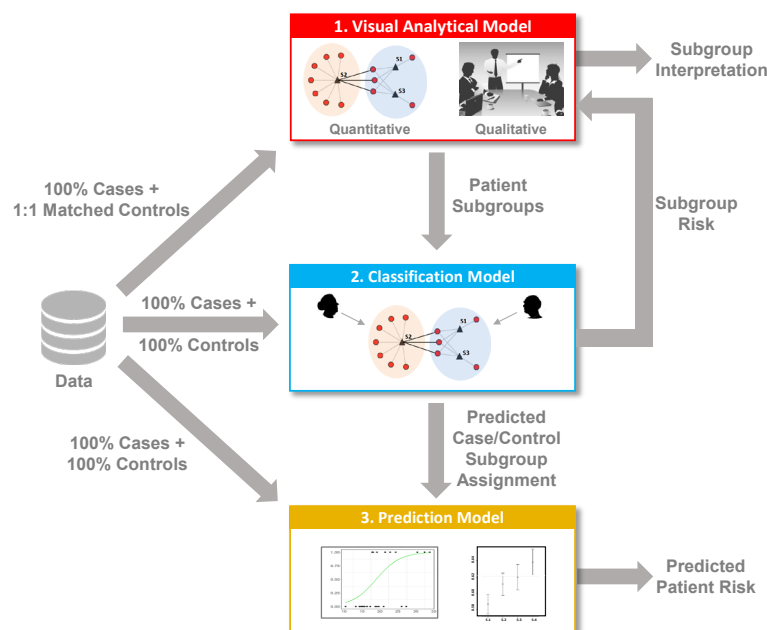


**Fig. 1.** Inputs and outputs for the three-step modeling in MIPS. The visual analytical model quantitatively identifies the patient subgroups, and visualizes them using a bipartite network. The classification model predicts subgroup membership of cases and controls in addition to the risk of each subgroup, which is juxtaposed with the visualization to enable clinicians to qualitatively interpret the readmission subgroups. The predictive model uses subgroup membership, comorbidities, and demographics to predict the risk of a new patient for being readmitted.

uses the subgroup membership assignment of cases and controls to predict the readmission risk of a patient. Appendix-1 (Table-1) provides a summary of the inputs, methods, and outputs from each model.

## Data Description

**Study population.** We analyzed patients hospitalized for chronic obstructive pulmonary disease (COPD), congestive heart failure (CHF), and total hip/knee arthroplasty (THA/TKA). We selected these three index conditions because: (a) hospitalizations for each of these conditions are highly prevalent in older adults [39]; (b) hospitals report very high variations in their readmission rates [39]; and (c) there exist well-tested readmission prediction models for each of these conditions that did not consider patient subgroups [42-44, 46, 47]. For each index condition, we used the same inclusion and exclusion criteria used to develop the CMS models, but with the most recent years (2013-2014) provided by Medicare when we started the project. Appendix-2 describes (1) the International Classification of Diseases, Ninth Version codes (ICD-9) codes for each of the three index conditions selected for analysis, and (2) the inclusion and exclusion criteria used to extract cases and controls for COPD, CHF, and THA/TKA, the respective numbers of patients extracted at each step, and how we addressed the small incidence of missing data. Each modeling method used relevant subsets of the above data, as described in the section on the analytical and evaluation approach.

**Variables.** The independent variables consisted of comorbidities, and patient demographics (age, gender, race). Comorbidities common in older adults were derived from three established comorbidity indices: Charlson Comorbidity Index (CCI) [48], Elixhauser Comorbidity Index (ECI) [49], and the Center for Medicare and Medicare Services Condition Categories (CMS-CC) used in the CMS readmission models [50] (the variables in the CMS models varied across the index conditions). As these indices had overlapping comorbidities, we derived a union of them, which was verified by the clinician stakeholders. They recommended that we also include the following additional variables as they were pertinent to each index condition: COPD (history of sleep apnea, mechanical ventilation); CHF (history of coronary artery bypass graft surgery); THA/TKA (congenital deformity of the hip joint, post-traumatic osteoarthritis). For each patient in our cohort, we extracted the above comorbidities and variables from the physicians, outpatient, and inpatient Medicare claims data in the 6 months before (to guard against miscoding), and on the day of the index admission. The dependent variable (outcome) was whether a patient with an index admission (COPD, CHF, THA/TKA) had an unplanned readmission to an acute-care hospital within 30 days of discharge, as was recorded in the MEDPAR file (inpatient claims) in the Medicare database.

## Analytical and Evaluation Approach

**Visual Analytical Modeling.** The goal of visual analytical modeling was to identify and interpret biclusters of readmitted patients (cases) consisting of patient subgroups and their most frequently co-occurring comorbidities. The data used to build the visual analytical model in each index condition consisted of randomly dividing 100% of the cases into a training (50%) and a replication (50%) dataset (we use the term *replication* to avoid confusion with the term *validation* typically used in classification and prediction models). For the feature selection, we extracted an equal number of 1:1 matched controls based on age, gender, and race/ethnicity, and Medicaid eligibility [51]. The above data were analyzed in each index condition using the following steps (Appendix-1 provides additional details for each step):

1. **Model Training.** To train the visual analytical model, we used feature selection for identifying the set of comorbidities that were univariably significant in both the training and replication datasets, and used bicluster modularity maximization [26, 27] for identifying the number, members, and significance of biclusters in the training dataset.
2. **Model Replication.** To test the replicability of the of biclusters, we repeated the above bicluster analysis on the replication dataset, and used the Rand Index (RI) [52] to measure the degree and significance of similarity in comorbidity co-occurrence between the two datasets.
3. **Model Interpretation.** To enable clinical interpretation of the patient subgroups, we used the *Fruchterman-Reingold* (FR) [29] and *ExplodeLayout* [30, 31] algorithms to visualize the network. Furthermore, based on a request from our clinician stakeholder team, for each bicluster we ranked and displayed the comorbidity labels with their univariable ORs for readmission (obtained from the feature selection above), and juxtaposed the

readmission risk of the bicluster (obtained from the classification step discussed below) onto the network visualization. Clinician stakeholders were asked to use the visualization to interpret the patient subgroups, their mechanisms, and potential interventions to reduce the risk for readmission.

**Classification Modeling.** The goal of the classification modeling was to classify all cases and controls from the entire Medicare dataset into the biclusters identified from the visual analytical model. The resulting bicluster membership for all cases and controls were designed to (a) develop the predictive modeling described below, and (b) measure the risk of each subgroup to enable clinical interpretation of the patient subgroups. The training dataset in each condition consisted of a random sample of 75% cases with their subgroup membership (output of the visual analytical modeling), and an internal validation dataset consisting of randomly selected 25% of the cases (with subgroup membership used to validate the model). The above data were used to develop and use classification models in each index condition using the following steps (Appendix-1 provides additional details for each step):

1. *Model Training.* To train the classifier, we used multinomial logistic regression [16] with independent variables consisting of comorbidities (identified through the feature selection). Accuracy of the trained model was measured by calculating the percentage of times the model correctly classified the cases into the subgroups, using the highest predicted probability across the subgroups.

2. *Model Internal Validation.* To internally validate the classifier, we randomly split the above data into the training (75%) and testing (25%) datasets, 1000 times. For each iteration, we trained a model using the training dataset, and measured its accuracy on the testing dataset. This was done by predicting the subgroup membership using the highest predicted probability among all the subgroups. The overall predicted accuracy was then estimated by calculating the mean accuracy across the 1000 models.

3. *Model Application.* To generate data for the visual analytical and prediction models, the above classifier was used to classify 100% cases and controls from our entire Medicare dataset (July 2013-August 2014). The resulting classified data were used to measure the risk of each subgroup risk (juxtaposed onto the network visualization to enable clinical interpretation), and to conduct the following prediction modeling.

**Prediction Modeling.** The goal of the prediction modeling was to predict the risk of readmission for a patient taking into consideration subgroup membership. The data used to build the prediction models consisted of 100% cases and 100% controls with subgroup membership generated from the above classification modeling. These data were randomly split into the training (75%) and validation (25%) datasets. The above data were used to train, internally validate, and compare prediction models in each index condition using the following steps (Appendix-1 provides additional details for each step):

1. *Model Training.* To train the prediction model, we used binary logistic regression for developing a Standard Model (without subgroup membership similar to the CMS models), and a Hierarchical Model (with subgroup membership). Independent variables for both models consisted of comorbidities (identified through the feature selection) and demographics, and the outcome was 30-day unplanned readmission (yes vs. no).

2. *Model Internal Validation.* To internally validate the models, we used the internal validation data set to measure discrimination (C-statistic), and calibration (calibration-in-the-large, and calibration slope).

3. *Model Comparisons.* To compare the accuracy of the Standard Model versus the Hierarchical Model, we used the chi-squared test to compare their C-statistics. Furthermore, to examine how the Standard Model performed on each subgroup, we measured the C-statistic of the Standard Model applied to each subgroup separately. Finally, because both of the above models used comorbidities selected through feature selection, they differed from the set of comorbidities used in the published CMS models. Therefore, to perform a head-to-head comparison with the published CMS models (COPD [42], CHF [43], and THA/TKA [44]), we developed a logistic regression model using the independent variables from the published CMS model (CMS Standard Model), and compared it to the same model but which also included subgroup membership (CMS Hierarchical Model). Similar to the above comparisons, we used the chi-squared test to compare the C-statistic of the CMS Standard Model versus the CMS Hierarchical Model, and additionally measured the differences between the models using Net Reclassification Improvement (NRI), Integrated Discrimination Improvement (IDI).

## RESULTS

### Data

Table 1 provides a summary of the number of cases and/or controls used to develop the three models in each condition.

### Visual Analytical Modeling

The visual analytical modeling of readmitted patients in all three index conditions produced statistically and clinically significant patient subgroups and their most frequently co-occurring comorbidities, which were significantly replicated. Results from each condition are described below.

**COPD.** The inclusion and exclusion selection criteria (see Appendix-2) resulted in a training dataset (n=14,508 matched case/control pairs, of which 51 patient pairs with no dropped comorbidities), and a replication dataset (n=14,508 matched case/control pairs, of which 51 patient pairs with no dropped comorbidities), matched by age, sex, race, and Medicaid eligibility (a proxy for economic status). The feature selection method (see Appendix-3) used 45 unique comorbidities identified from a union of the three comorbidity indices, plus 2 condition-specific comorbidities. Of these, 3 were removed because of <1% prevalence. Of the remaining, 30 survived the significance and replication testing with Bonferroni correction. The visual analytical model used these surviving comorbidities (d=30), and cases consisting of CHF readmitted patients with at least one of those comorbidities (n=14,457). As shown in Fig. 2, the bipartite network analysis identified 4 biclusters, each representing a subgroup of readmitted COPD patients and their most frequently co-occurring comorbidities. The biclustering had significant modularity ( $Q=0.17$ ,  $z=7.3$ ,  $P<.001$ ), and significant replication ( $RI=0.92$ ,  $z=11.62$ ,  $P<.001$ ) of comorbidity co-occurrence. Furthermore, as requested by the clinician stakeholders, we juxtaposed a ranked list of comorbidities based on their ORs for readmission in each bicluster, in addition to the risk for each of the patient subgroups.

The pulmonologist inspected the visualization and noted that the readmission risk of the patient subgroups had a wide range (12.7% to 19.6%) with clinical (face) validity. Furthermore, the co-occurrence of comorbidities in each patient subgroup was clinically meaningful with interpretations for each subgroup. Subgroup-1 had a low disease burden with uncomplicated hypertension leading to the lowest risk (12.7%). This subgroup represented patients with early organ dysfunction and would benefit from using checklists such as regular monitoring of blood pressure in pre-discharge protocols to reduce the risk of readmission. Subgroup-3 had mainly psychosocial comorbidities, which could lead to aspiration precipitating pneumonia leading to an increased risk for readmission (15.9%). This subgroup would benefit from early consultation with specialists (e.g., psychiatrists, therapists, neurologists, and geriatricians) that had expertise in psycho-social comorbidities, with a focus on the early identification of aspiration risks and precautions. Subgroup-2 had diabetes with complications, renal failure and heart failure and therefore had higher disease burden leading to an increased risk for readmission (17.8%) compared to Subgroup-1. This subgroup had metabolic abnormalities with greater end-organ dysfunction and would therefore benefit from case management from advanced practice providers (e.g., nurse practitioners) with rigorous adherence to established guidelines to reduce the risk of readmission. Subgroup-4 had diseases with end-organ damage including gastro-intestinal disorders, and therefore had the highest disease burden and risk for readmission (19.6%). This subgroup would also benefit from case management with rigorous adherence

Model	Training	Replication/ Validation	Total
<b>Visual Analytical*</b>			
COPD (cases/controls)	14,508/14,508	14,508/14,508	29,016/29,016
CHF (cases/controls)	25,775/25,775	25,775/25,775	51,550/51,550
THA/TKA (cases/controls)	8,249/8,249	8,249/8,249	16,498/16,498
<b>Classification</b>			
COPD (cases)	10,842	3,615	14,457
CHF (cases)	19,254	6,418	25,672
THA/TKA (cases)	5,257	1,753	7,010
<b>Prediction</b>			
COPD (cases/controls)	21,692/117,839	7,334/39,176	29,026/157,015
CHF (cases/controls)	38,728/183,093	12,845/61,095	51,573/244,188
THA/TKA (cases/controls)	12,376/255,203	41,44/85,049	16,520/340,252

**Table 1.** Training and replication/validation datasets used to develop the three models in each of the three index conditions.

\*The visual analytical models used 1:1 matched controls for the feature selection, and used only cases for the bipartite networks to analyze heterogeneity in readmission. The numbers shown for the visual analytical models are before removing patients with no comorbidities. The resulting cases-only datasets were used for the classification modelling as shown.

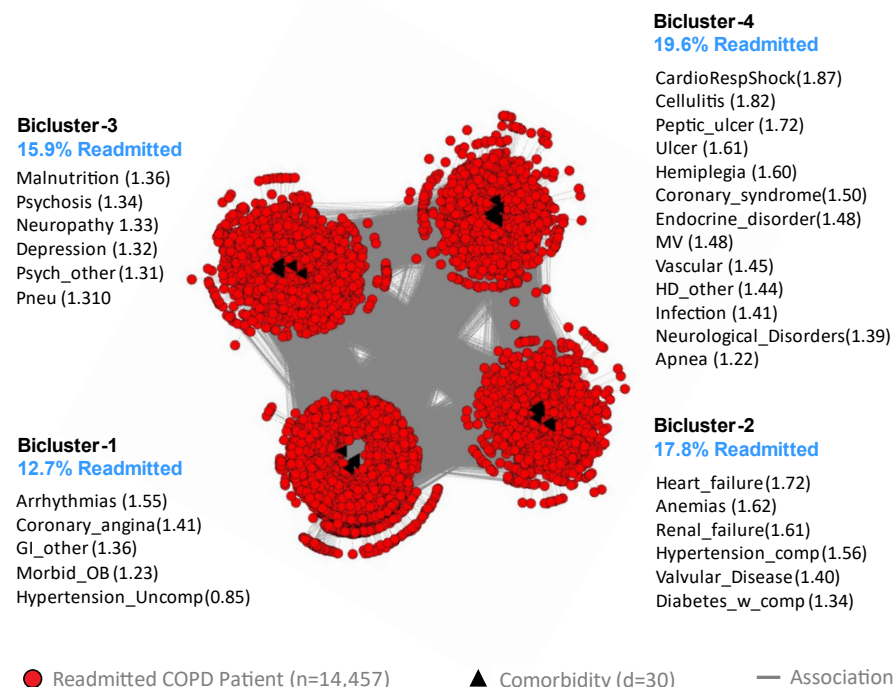


**Fig. 2.** The COPD visual analytical model showing four biclusters consisting of patient subgroups and their most frequently co-occurring comorbidities (whose labels are ranked by their univariable ORs, shown within parentheses), and their risk of readmission (shown in blue text).

Abbreviations: CardioRespShock, cardiorespiratory shock; COPD, chronic obstructive pulmonary disease; GI, gastrointestinal; Id, identifier; OB, obesity; Pneu, pneumonia; Psych, psychiatric; Uncomp, uncomplicated; HD\_other, other and unspecified heart disease; MV, history of mechanical ventilation.

to established guidelines to reduce the risk of readmission. Furthermore, as patients in this subgroup typically experience complications that could impair their ability to make medical decisions, they should be provided with early consultation with a palliative care team to ensure that care interventions align with patients' preferences and values.

**CHF.** The inclusion and exclusion selection criteria (see Appendix-2) resulted in a training dataset (n=25,775 matched case/control pairs, of which 103 patient pairs with no dropped comorbidities) and a replication dataset (n=25,775 matched case/control pairs, of which 104 patient pairs with no dropped comorbidities), matched by age, sex, race, and Medicaid eligibility (a proxy for economic status). The feature selection method (see Appendix-3) used 42 unique comorbidities identified from a union of the three comorbidity indices, plus 1 condition-specific comorbidity. Of these, 1 comorbidity was removed because of <1% prevalence. Of those remaining, 37 survived the significance and replication testing with Bonferroni correction. The visual analytical model (Fig. 4) used these surviving comorbidities (d=37), and cases consisting of CHF readmitted patients with at least one of those comorbidities (n=25,672). As shown in Fig. 3, the bipartite network analysis of the CHF cases identified 4 biclusters, each representing a subgroup of readmitted CHF patients and their most frequently co-occurring comorbidities. The analysis revealed that the biclustering had significant modularity ( $Q=0.17$ ,  $z=8.69$ ,  $P<.001$ ), and significant replication ( $RI=0.94$ ,  $z=17.66$ ,  $P<.001$ ) of comorbidity co-occurrence. Furthermore, as requested by the clinicians, we juxtaposed a ranked list of comorbidities based on their ORs for readmission in each bicluster, in addition to the risk for each of the patient subgroups.

The geriatrician inspected the visualization and noted that the readmission risk of the patient subgroups, ranging from 15.1% to 19.9%, was wide with clinical (face) validity. Furthermore, the co-occurrence of comorbidities in each patient subgroup was clinically meaningful. Subgroup-1 had chronic but stable conditions, and therefore had the lowest risk for readmission (15.1%). Subgroup-3 had mainly psychosocial comorbidities, but were not as clinically unstable or fragile compared to subgroups 2 and 4, and therefore had medium risk (16.6%). Subgroup-

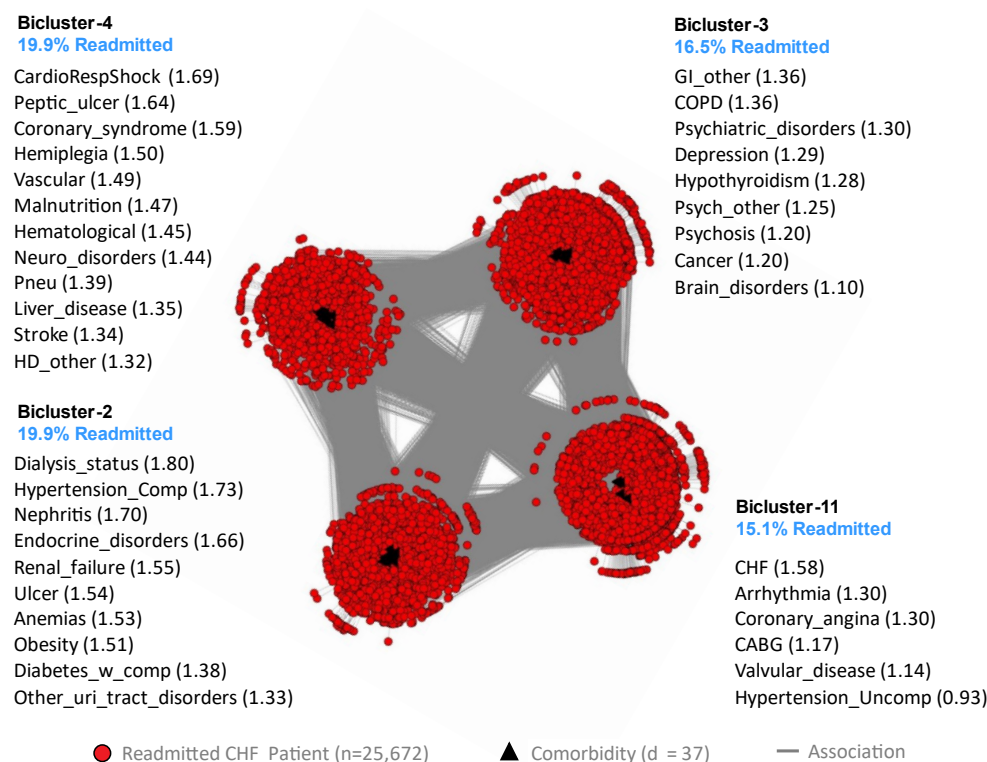


**Fig. 3.** The CHF visual analytical model showing four biclusters consisting of patient subgroups and their most frequently co-occurring comorbidities (whose labels are ranked by their univariable ORs, shown within parentheses), and their risk of readmission (shown in blue text).

Abbreviations: CABG, coronary artery bypass graft; CardioRespShock, cardiorespiratory shock; CHF, congestive heart failure; comp, complicated; COPD, chronic obstructive pulmonary disease; GI, gastrointestinal; Id, identifier; Neuro, neurologic; OB, obesity; Pneu, pneumonia; Psych, psychiatric; Uncomp, uncomplicated; uri, urinary; w\_comp, with complications; HD\_other, other and unspecified heart disease.

2 had severe chronic conditions, making them clinically fragile (with potential benefits from early palliative and hospice care referrals), and were therefore at high risk for readmission if non-palliative approaches were used (19.9%). Subgroup-4 had severe acute conditions which were also clinically unstable, associated with substantial disability and care debility, and therefore at high risk for readmission and recurrent intensive care unit (ICU) use (19.9%).

**THA/TKA.** The inclusion and exclusion selection criteria (see Appendix-2) resulted in a training dataset (n=8,249 matched case/control pairs, of which 1239 patient pairs with no dropped comorbidities) and a replication dataset (n=8,249 matched case/control pairs, of which 1264 patient pairs with no dropped comorbidities), matched by age, sex, race, and Medicaid eligibility (a proxy for economic status). The feature selection (see Appendix-3) used 39 unique comorbidities identified from the three comorbidity indices plus 2 condition-specific comorbidities. Of these, 11 comorbidities were removed because of <1% prevalence. Of the remaining, 11 survived the significance and replication testing with Bonferroni correction. The visual analytical model (Fig. 5) used these surviving comorbidities (d=11), and cases consisting of readmitted patients with at least one of those comorbidities (n=7,010).

As shown in Fig. 4, the bipartite network analysis of the THA/TKA cases identified 7 biclusters, each representing a subgroup of readmitted THA/TKA patients and their most frequently co-occurring comorbidities. The analysis revealed that the biclustering had significant modularity ( $Q=0.31$ ,  $z=2.52$ ,  $P=.011$ ), and significant replication ( $RI=0.89$ ,  $z=3.15$ ,  $P=.002$ ) of comorbidity co-occurrence. Furthermore, as requested by the clinician stakeholders,

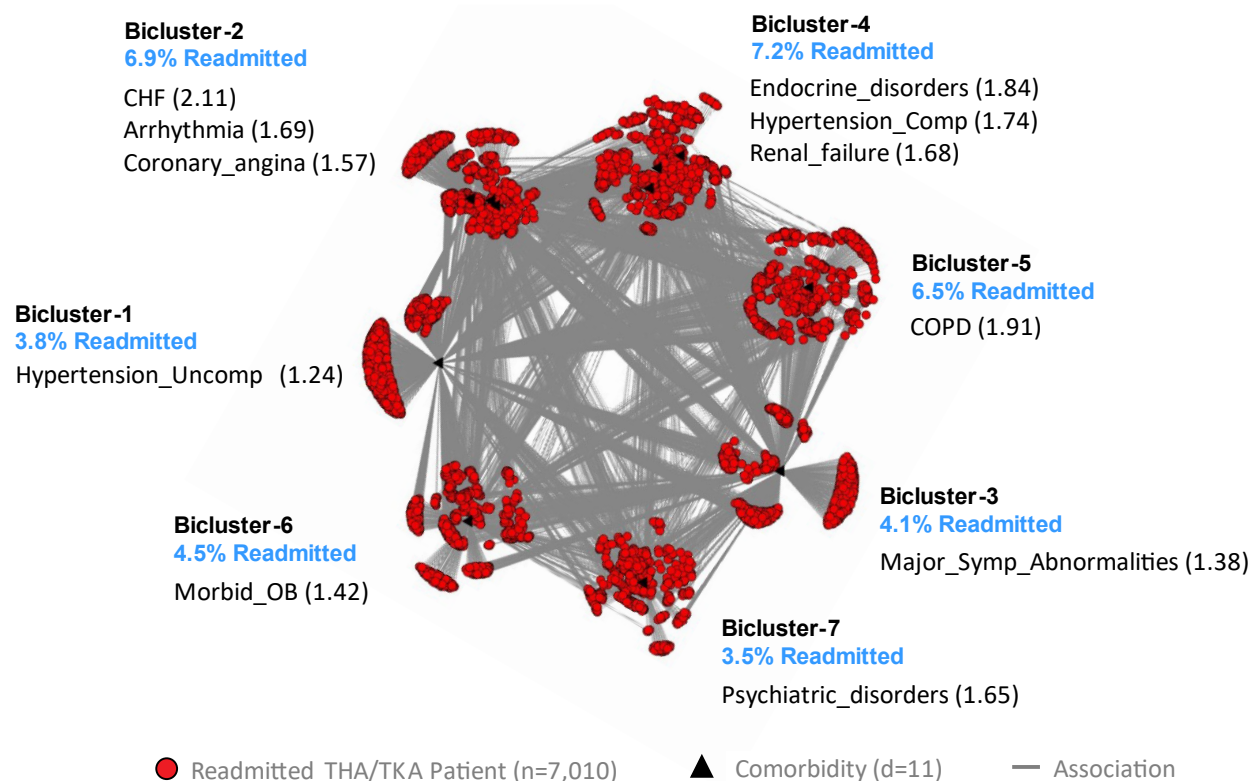


**Fig. 4.** The THA/TKA visual analytical model showing four biclusters consisting of patient subgroups and their most frequently co-occurring comorbidities (whose labels are ranked by their univariable ORs, shown within parentheses), and their risk for readmission (shown in blue text).

Abbreviations: CHF, congestive heart failure; comp, complicated; COPD, chronic obstructive pulmonary disease; Id, identifier; OB, obesity; Symp, symptom; THA/TKA, total hip/knee arthroplasty; Uncomp, uncomplicated.

we juxtaposed a ranked list of comorbidities based on their ORs for readmission in each bicluster, in addition to the risk for each of the patient subgroups.

The geriatrician inspected the network and noted that TKA patients, in general, were healthier compared to THA patients, and therefore the network was difficult to interpret when the two index conditions were merged together. While our analysis was constrained because we were using the conditions as defined by CMS, these results nonetheless suggest that the interpretations did not suffer from a confirmation bias (manufactured interpretations to fit the results). However, he noted that the range of readmission risk had clinical (face) validity. Furthermore, subgroups 2, 4, and 5 had more severe comorbidities related to lung, heart, and kidney, and therefore had a higher risk for readmission compared to subgroups 1, 6, and 7 that had less severe comorbidities with a lower risk for readmission. In addition, subgroups 2, 5, 6 and 7 would benefit from chronic care case management from advanced practice providers (e.g., nurse practitioners). Finally, subgroups 2 and 5 could benefit from using well-established guidelines for CHF and COPD, subgroup 7 would benefit from mental health care and management of psycho-social comorbidities, and subgroup 6 would benefit from care for obesity and metabolic disease management.

## Classification Modeling

The classification model used multinomial logistic regression in each index condition (see Appendix-4 for the model coefficients) to predict the membership of patients using subgroups (identified from the above visual analytical models). The results revealed that in each index condition, the classification model had high accuracy in classifying all the cases in the full dataset (training dataset used in the visual analytical modeling). Similarly, the internal validation results using a 75%-25% split of the above dataset also had high classification accuracy (Table 2 with classification accuracy divided into quantiles). We report both results for each index condition:

**COPD.** The model correctly predicted subgroup membership for 99.90% of the cases (14443/14457) in the full dataset. Furthermore, as shown in Table 2, the internal validation results revealed that the percentage of COPD cases correctly assigned to a subgroup in the testing dataset, ranged from 99.10% to 100.00%, with a median (Q.50) of 99.60%, and with 95% being in the range from 99.30% to 99.80%.

**CHF.** The model correctly predicted subgroup membership for 99.20% of the cases (25476/25672) in the full dataset. Furthermore, as shown in Table 3, the internal validation results revealed that the percentage of CHF cases correctly assigned to a subgroup in the testing dataset, ranged from 98.70% to 99.70%, with a median (Q.50) of 99.30%, and with 95% being in the range from 99.00% to 99.60%.

**THA/TKA.** The model correctly predicted subgroup membership 100.00% of the cases (7010/7010) in the full dataset. Furthermore, as shown in Table 2, the internal validation results revealed that the percentage of CHF cases correctly assigned to a subgroup in the testing dataset, ranged from 99.40% to 100.00%, with a median (Q.50) of 99.90%, and with 95% being in the range from 99.70% to 100.00%.

Models	Quantiles					Summary			
	Q .025	Q .25	Q .50	Q .75	Q .975	Min	Max	Mean	SD
<b>COPD</b>									
Training (n=10842)	99.90	100.00	100.00	100.00	100.00	99.70	100.00	100.00	0.02
Testing (n=3615)	99.30	99.40	99.60	99.60	99.80	99.10	100.00	99.60	0.15
<b>CHF</b>									
Training (n=19254)	99.40	99.50	99.60	99.60	99.80	99.00	99.90	99.57	0.11
Testing (n=6418)	99.00	99.30	99.30	99.40	99.60	98.70	99.70	99.34	0.15
<b>THA/TKA</b>									
Training (n=5257)	100.00	100.00	100.00	100.00	100.00	100.00	100.00	100.00	0.00
Testing (n=1753)	99.70	99.80	99.90	99.90	100.00	99.40	100.00	99.86	0.09

**Table 2.** Internal validation results showing the percentage of COPD, CHF, and THA/TKA patients correctly-assigned to a subgroup by the classification models in each condition.

**Application of the Classification Model to Generate Information for Other Models.** The above classification model was used to classify 100% cases and 100% controls for use in the prediction model (described below). Furthermore, the proportion of cases and controls classified into each subgroup was used to calculate the risk of readmission for each subgroup (see Appendix-3). As this subgroup risk information was requested by the clinicians to improve interpretability of the visual analytical model, the values were juxtaposed next to the respective subgroups in the bipartite network visualizations (see blue text in Fig. 3-5).

## Prediction Modeling

For each of the three index conditions, we developed two binary logistic regression models to predict readmission, with comorbidities in addition to sex, age, and race: (1) **Standard Model** representing all patients without subgroup membership, similar to the CMS models; and (2) **Hierarchical Model** with an additional variable that adjusted for subgroup membership.

**COPD.** The inclusion and exclusion selection criteria (see Appendix-2) resulted in a cohort of 186,041 patients (29,026 cases and 157,015 controls). As shown in Fig. 5A, the Standard Model had a C-statistic of 0.624 (95% CI: 0.617-0.631) which was not significantly ( $P=.8578$ ) different from the Hierarchical Model that had a C-statistic of 0.625 (95% CI: 0.618-0.632). The calibration plots revealed that both models had a slope close to 1, and an intercept close to 0 (see Appendix-5).

As shown in Fig. 6B, the Standard Model was used to measure the predictive accuracy of patients in each subgroup separately. The results showed that Subgroup-1 had a lower C-statistic compared to Subgroup-3 and Subgroup-4. While the C-statistics in Fig. 5A and Fig. 5B cannot be compared as they are based on models developed from different populations, these results reveal that the current CMS readmission model for CHF might be underperforming for one COPD patient subgroup, pinpointing which one might benefit by a Subgroup-Specific Model.

**CHF.** The inclusion and exclusion selection criteria (see Appendix-2) resulted in a cohort of 295,761 patients (51,573 cases and 244,188 controls). As shown in Fig. 6A, the Standard Model had a C-statistic of 0.600 (95% CI: 0.595-0.605), which was not significantly different ( $P=0.2864$ ) from the Hierarchical Model that also had a C-statistic of 0.600 (95%CI: 0.595-0.605). The calibration plots revealed that all models had a slope close to 1, and an intercept close to 0 (see Appendix-5).

As shown in Fig. 6B, the Standard Model was used to measure the predictive accuracy of patients in each subgroup separately. The results showed that Subgroup-1 had a lower C-statistic compared to Subgroup-4. While the C-statistics in Fig. 6A and Fig. 6B cannot be compared as they are based on models developed from different populations, but similar to the results in COPD, these results reveal that the current CMS readmission model for CHF might be underperforming for one CHF patient subgroup, pinpointing which one might benefit by a Subgroup-Specific Model.

**THA/TKA.** The application of the inclusion and exclusion selection criteria (see Appendix-2) resulted in a cohort of 356,772 patients (16,520 cases and 340,252 controls). As shown in Fig. 7A, the Standard Model had a C-statistic of 0.638 (95% CI: 0.629-0.646), which was not significantly different ( $P=0.6817$ ) from the Hierarchical Model that had a C-statistic of 0.638 (95% CI: 0.629-0.647). The calibration plots (see Appendix-5) revealed that both models had a slope close to 1, and an intercept close to 0 (see Appendix-5).

As shown in Fig. 7B, the Standard Model was used to measure the predictive accuracy of patients in each subgroup separately. The results showed that Subgroup-1 had a lower C-statistic compared to Subgroup-4. Again, while the C-statistics in Fig. 7A and Fig. 7B cannot be compared as they are based on models developed from different populations, similar to the results in COPD, these results reveal that the current CMS readmission model for THA/TKA might be underperforming for 4 patient subgroups, pinpointing which ones might benefit by Subgroup-Specific Models.

#### CMS Standard Model vs. CMS Hierarchical Model.

Unlike the CMS published models, the above models used only the comorbidities that survived feature selection. Therefore, to perform a head-to-head comparison with the published CMS models, we also developed a CMS Standard Model (using the same variables from the published CMS model), and compared it to the corresponding CMS Hierarchical Model (with an additional variable for subgroup membership) in each condition. Similar to the models in Fig. 5-7, there were no significant

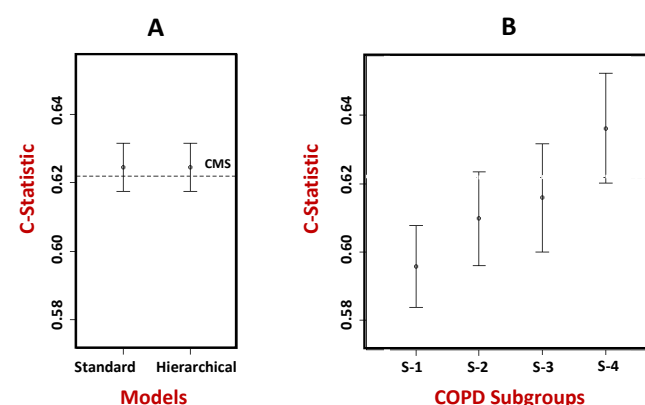


**Fig. 5. (A)** Predictive accuracy of the Standard Model compared to the Hierarchical model in COPD, as measured by the C-Statistic. The C-statistic for the CMS published model is shown as a dotted line. **(B)** Predictive accuracy of the Standard Model when applied separately to patients classified to each subgroup. S-1 has lower accuracy compared to S-3 and S-4. (C-statistics in A and B cannot be compared as they are based on models from different populations).

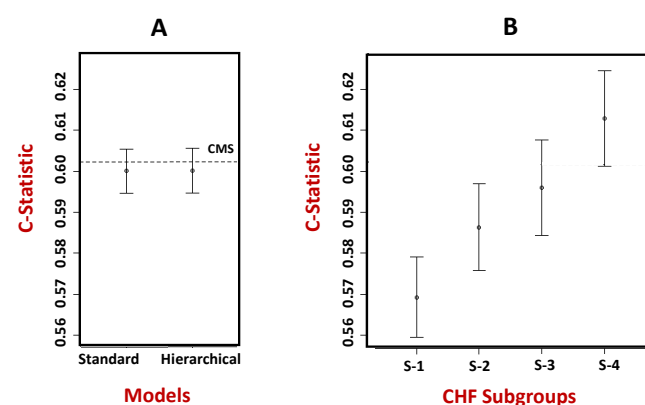


**Fig. 6. (A)** Predictive accuracy of the Standard Model compared to the Hierarchical model in CHF as measured by the C-Statistic. The C-statistic for the CMS published model is shown as a dotted line. **(B)** Predictive accuracy of the Standard Model when applied separately to patients classified to each subgroup. S-1 has lower accuracy compared to S-3 and S-4. (C-statistics in A and B cannot be compared as they are based on models from different populations).

differences in the C-statistics between the two modeling approaches in any condition (see Appendix-5). However, as shown in Table 3, the CMS Hierarchical Model for COPD had significantly higher NRI, but not significantly higher NDI compared to the CMS Standard Model; the CMS Hierarchical Model for CHF had a significantly lower NRI and IDI compared to the CMS Standard Model, and the CMS Hierarchical Model for THA/TKA had a significantly higher NDI and IDI compared to the CMS Standard Model. Furthermore, similar to the results in 6B-8B, when the CMS Standard Model was used to predict readmission separately in subgroups within each index condition, it identified subgroups that underperformed, pinpointing which ones might benefit by a Subgroup-Specific Model (See Appendix-5). In summary, the comparisons between the CMS Standard Models and the respective CMS Hierarchical Models showed that in two conditions (COPD and THA/TKA), there was a small but statistically significant improvement in discriminating between the readmitted and not readmitted patients as measured by NRI, but not as measured by the C-statistic or IDI, and that a subgroup in each index condition might be underperforming when using the CMS Standard Model.

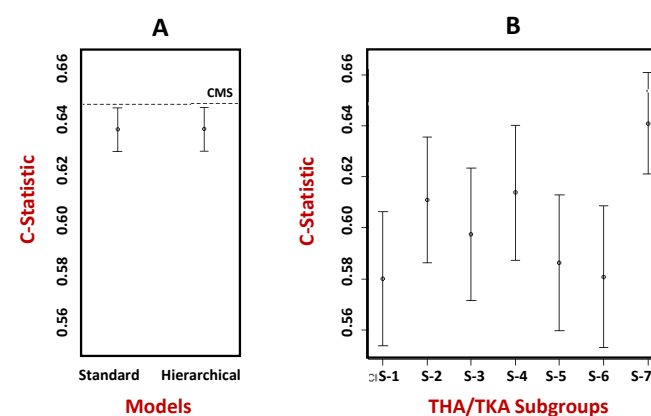


**Fig. 7. (A)** Predictive accuracy of the Standard Model compared to the Hierarchical model in THA/TKA as measured by the C-Statistic. The C-statistic for the CMS published model is shown as a dotted line. **(B)** Predictive accuracy of the Standard Model when applied separately to patients classified to each subgroup. S-1 has lower accuracy compared to S-7. (C-statistics in A and B cannot be compared as they are based on models developed from different populations).

Model	NRI		IDI
	Categorical (95% Interval)	Continuous (95% Interval)	IDI (95% Interval)
COPD	.023 (.012, .034)*	.059 (.034, .083)*	.0002 (-.0004, .0008)
CHF	-.010 (-.016, -.0004)*	-.038 (-.057, -.019)*	-.0006(-.0009,- .0003)*
THA/TKA	.022 (.012, .032)*	.111 (.080, .142)*	-.003(-.002,- .003)*

**Table 3.** Comparison of the CMS Standard Model with the CMS Hierarchical Model across the three index conditions based on NRI and IDI (\* = significant at the .05 level).

## DISCUSSION

### Overview

Our overall approach of using the MIPS framework to identify patient subgroups through visual analytics, and using those subgroups to build classification and prediction models, revealed strengths and limitations for each modeling approach, and for our data source. This examination led to insights for developing future clinical decision support systems, and a methodological framework for improving the clinical interpretability of subgroup modeling results.

### Strengths and Limitations of Modeling Methods and Data Source

**Visual Analytical Modeling.** The results revealed three strengths of the visual analytical modeling: (1) the use of bipartite networks to simultaneously model patients and comorbidities, enabled the automatic identification of patient-comorbidity biclusters, and the integrated analysis of co-occurrence and risk; (2) the use of a bipartite modularity maximization algorithm to identify the biclusters enabled the measurement of the strength of the biclustering, critical for gauging its significance; and (3) the use of a graph representation enabled the results to be visualized through a network. Furthermore, the request from the clinician stakeholders to juxtapose the risk of each subgroup with their visualizations appeared to be driven by a need to reduce working memory loads (from having to remember that information spread over different outputs), which could have enhanced their ability to match bicluster patterns with chunks (previously-learned patterns of information) stored in long-term

memory. The resulting visualizations enabled them to recognize subtypes based on co-occurring comorbidities in each subgroup, reason about the processes that precipitate readmission based on the risk of each subtype relative to the other subtypes, and propose interventions that were targeted to those subtypes and their risks. Finally, the fact that the geriatrician could not fully interpret the THA/TKA network because it mixed two fairly different conditions, suggests that the clinical interpretations were not the result of a *confirmation bias* (interpretations leaning towards fitting the results).

However, the results also revealed two limitations: (1) while modularity is estimated using a closed-form equation (formula), no closed-form equation exists to estimate the modularity variance, which is necessary to measure its significance. To estimate modularity variance, we therefore used a permutation test by generating 1000 random permutations of the data, and then compared the modularity generated from the real data to the mean modularity generated from the permuted data. Given the size of our datasets (ranging from 7K-25K patients), this computationally-expensive test took approximately 7 days to complete, despite the use of a dedicated server with multiple cores; and (2) while bicluster modularity was successful in identifying significant and meaningful patient-comorbidity biclusters, the visualizations themselves were extremely dense, and therefore potentially concealed patterns within and between the subgroups. Future research should explore a closed-form equation to estimate modularity variance, with the goal of accelerating the estimation of modularity significance, and more powerful analytical and visualization methods to reveal intra- and inter-cluster associations in large and dense networks.

Classification Modeling. The results revealed two strengths of the classification modeling: (1) the use of a simple multinomial classifier was adequate to predict with high accuracy to which subgroup a patient belonged; (2) because the model produced membership probabilities for each patient for each subgroup, the model captured the dense inter-cluster edges observed in the network visualization; and (3) the coefficients of the trained classifier could be inspected by an analyst making it more transparent (relative to most deep-learning classifiers which tend to be a black box).

However, because we dichotomized the classification probabilities into a single subgroup membership, our approach did not fully leverage the membership probabilities for modeling and visual interpretation. For example, some patients have high classification probabilities (representing strong membership) to a single subgroup (as shown by patients in the outer periphery of the biclusters with edges only within their bicluster), whereas others have equal probabilities to all subgroups (as shown in the inner periphery of the biclusters with edges going to multiple clusters). Future research should explore incorporating the probability of subgroup membership into the design of hierarchical models to improve predictive accuracy, and visualization methods to help clinicians interpret patients with different profiles of membership strength, with the goal of designing patient-specific interventions.

Predictive Modeling. The results revealed two strengths of the predictive modeling: (1) the use of the Standard Model to measure predictive accuracy across the subgroups helped to pinpoint which subgroups tend to have lower predictive accuracy compared to the rest, and therefore which of them could benefit from a more complex but accurate subgroup-specific model; and (2) despite the use of a simple Hierarchical Model with a dichotomized membership label for each patient, the predictive CMS models detected significant differences in the prediction accuracy as measured by NRI in two of the conditions, when compared to the CMS Standard Models. However, the results also revealed that the differences in predictive accuracy as measured by the C-statistic and NDI were small, suggesting that comorbidities on their own were potentially insufficient for accurately predicting readmission. Future research should explore the use of electronic health records, and the use of multiple subgroup-specific models targeted to each subgroup (enabling each model to have different slopes and intercepts), to potentially improve the predictive accuracy of the prediction models.

Data Source. The Medicare claims data had four key strengths: (1) scale of the datasets which enabled subgroup identification with sufficient statistical power; (2) spread of the data collected from across the US which enabled generalizability of the results; (3) data about older adults which enabled examination of subgroups in an underrepresented segment of the US population; and (4) data used by CMS to build predictive readmission models, which enabled a head-to-head comparison with the hierarchical modeling approach.

However, the data had two critical limitations. (1) As we compared our models with the CMS models, we had to use the same definition for controls (90 days with no readmission) that had been used, which introduced a selection bias that exaggerates the separation between cases and controls. Similarly, by excluding patients who died, this exclusion criterion potentially biased the results towards healthier patients. (2) Administrative data have known limitations such as the lack of comorbidity severity and test results, which could strongly impact the accuracy of predictive models. Future research should consider the use of national-level electronic health record (EHR) data such as those being assembled by the National COVID Cohort Collaborative (N3C) [53], and the TriNetX [54] initiatives, which could overcome the above limitations by providing laboratory values and comorbidity severity, but could also introduce new as yet unknown limitations.

### **Implications for Clinical Decision-Support that Leverage Patient Subgroups**

While the focus of this project was to develop and evaluate the MIPS framework, its application to three index conditions coupled with extensive discussions with clinicians led to insights for designing a future clinical decision support system. Such a system could integrate outputs from all three models in MIPS. As we have shown, the visual analytical model automatically identified and visualized the patient subgroups, which enabled the clinicians to comprehend the co-occurrence and risk information in the visualization, reason about the processes that lead to readmission in each subgroup, and design targeted interventions. The classification model leveraged the observation that many patients have comorbidities in other biclusters (shown by a large number of edges between biclusters), and accordingly generated a membership probability of a patient belonging to each bicluster, from which the highest was chosen for bicluster membership. Finally, the predictive model predicts the risk for readmission for a patient, by using in the future the most accurate model designed for the bicluster to which the patient belongs.

The outputs from the above models could be integrated into a clinical decision support system to provide recommendations for a specific patient using the following algorithm: (1) use the classifier to generate the membership probability (MP) of a new patient belonging to each subgroup; (2) multiply the MP in each subgroup with the patient's risk (R) for readmission provided by the predictive model for that subgroup, to generate an importance score [ $IS = f(MP) \times g(R)$ ] for the respective intervention; (3) rank the subgroups and their respective interventions using IS; and (4) use the ranking to display in descending order, the subgroup comorbidity profiles along with their respective potential mechanisms, recommended treatments, and the respective IS. Such model-based information, displayed through a user-friendly interface, could enable a clinician to rapidly scan the ranked list to (a) determine why a specific patient's profile fits into one or more subgroups, (b) review the potential mechanisms and interventions ranked by their importance, and (c) use the combined information to design a treatment that is customized for the real-world context of the patient. Consequently, such a clinical decision support system could not only provide a quantitative ranking of membership to different subgroups, and the importance score for the associated interventions, but also enable the clinician to understand the rationale underlying those recommendations, making the system interpretable and explainable. Comparative evaluation of such a system to standard care could determine its clinical efficacy.

### **Implications for Analytical Granularity to Enhance the Interpretability of Patient Subgroups**

While the visual analytical model enabled the clinicians to interpret the patient subgroups, they were unable to interpret the associations within and between the subgroups due to the large number of nodes in each bicluster and the dense edges between them. Several network filtering methods [55, 56] have been developed to "thin out" such dense networks such as by dropping or bundling nodes and edges based on user-defined criteria, to improve visual interpretation. However, such filtering could bias the results, or modify the clusters resulting from the reduced data.

An alternate approach that preserves the full dataset leverages the notion of analytical granularity, where the data is progressively analyzed at different levels. For example, we have analyzed COVID-19 patients [11] at the cohort, subgroup, and patient levels, and we are currently using the same approach to examine symptom co-occurrence and risk at each level in Long COVID patients. Our preliminary results suggest that analyzing data at different levels of granularity enables clinicians to progressively interpret patterns such as within and between subgroups, in addition to guiding the systematic development of new algorithms. For example, at the subgroup

level, we have designed an algorithm that identifies which patient subgroups have a significantly higher probability for having characteristics that are clustered in another subgroup, providing critical information to clinicians about how to design interventions for such overlapping subgroups; at the patient level, we have identified patients that are outliers to their subgroups based on their pattern of characteristics inside and outside their subgroup. Such patient outliers could be flagged to examine if they need individualized interventions versus those recommended for the rest of their subgroup. Such analytical granularity could therefore inform the design of interventions by clinicians, in addition to the design of decision support systems that provide targeted and interpretable recommendations to physicians, who can then customize them to fit the real-world context of a patient.

## Implications of the MIPS Framework for Precision Medicine

While we have demonstrated the application of the MIPS framework across multiple readmission conditions, its architecture has three properties that should enable its generalizability across other medical conditions. First, as shown in Fig. 2, the framework is *modular* with explicit inputs and outputs, enabling the use of other methods at each of the three modeling steps. For example, the framework could use other biclustering (e.g., Non-negative Matrix Factorization [57]), classification (e.g., deep learning [58]), and prediction methods (e.g., subgroup-specific modeling [16]). Second, the framework is *extensible*, enabling an elaboration of the methods at each modeling step to improve the analysis and interpretation of subgroups. For example, as discussed above, the analytical granularity at the cohort, subgroup, and patient levels could improve the interpretability of subgroups in large and dense datasets. Third, the framework is *integrative* as it systematically combines the strengths of machine learning, statistical, and precision medicine approaches. For example, the visual analytical modeling leverages search algorithms to discover co-occurrence in large datasets; the classification and prediction modeling leverages probability theory to measure the risk of co-occurrence patterns; and clinicians leverage medical knowledge and human cognition to interpret patterns of co-occurrence and risk for designing precision-medicine interventions. Such integration of different models and their interpretation operationalizes *team-centered informatics* [59] designed to facilitate data scientists, biostatisticians, and clinicians in multidisciplinary translational teams [60] to work more effectively across disciplinary boundaries, with the goal of designing interventions for precision medicine. Our current research tests the generality of the MIPS framework in other conditions such as Long COVID and Post-Stroke Depression, with the goal of designing and evaluating precision medicine interventions targeted to patient subgroups.

## CONCLUSIONS

Although several studies have identified patient subgroups in different conditions, there is a considerable gap between the identification of subgroups, and their modeling and interpretation for clinical applications. Here we developed MIPS, a novel analytical framework to bridge that gap using a three-step modeling approach. A visual analytical method automatically identified statistically significant and replicated patient subgroups and their frequently co-occurring comorbidities. Next, a multinomial logistic regression classifier had high accuracy in correctly classifying patients into the patient subgroups identified by the visual analytical model. Finally, despite using a simple hierarchical logistic regression model to incorporate subgroup information, the predictive models had a statistically significant improvement in discriminating between the readmitted and not readmitted patients in two of the three readmission conditions, and additional analysis pinpointed for which patient subgroups the current CMS model might be underperforming. Furthermore, the integration of the three models helped to (1) elucidate the data input and output dependencies among the models enabling clinicians to interpret the patient subgroups, reason about mechanisms precipitating hospital readmission, and design targeted interventions, and (2) provide a generalizable framework for the development of future clinical decision support systems that integrate outputs from each of the three modeling approaches.

However, evaluation MIPS across three readmission index conditions also helped to identify limitations of the models and the data. The visual analytical model was too dense to enable the clinicians to interpret the associations within and between the subgroups, and the absence of a closed-form equation to measure modularity variance required a computationally-expensive process to measure the significance of the

biclustering. Furthermore, the small improvement in predictive accuracy suggested that comorbidities on their own were insufficient for predicting hospital readmission.

By leveraging the modular and extensible nature of the MIPs framework, future research should address the above limitations by developing more powerful algorithms which analyze subgroups at different levels of granularity to improve the interpretability of intra- and inter-cluster associations, and the evaluation of subgroup-specific models to predict outcomes. Furthermore, EHR data made available through national-level data initiatives such as N3C and TriNetX now provide access to critical variables including laboratory results and comorbidity severity, which should lead to higher predictive power for predicting adverse outcomes. Finally, extensive discussions with clinicians have confirmed the need for decision support systems which integrate outputs from the three models to provide for a specific patient, predicted subgroup memberships, ranked interventions, along with associated subgroup profiles and mechanisms. Such interpretable and explainable systems could enable clinicians to use patient subgroup information for informing the design of precision medicine interventions, with the goal of reducing adverse outcomes such as unplanned hospital readmissions and beyond.

## ACKNOWLEDGEMENTS

We thank Tianlong Chen, Clark Andersen, Yu-Li Lin, and Emmanuel Santillana for helping to conduct the analyses. This study was supported in part by the Patient-Centered Outcomes Research Institute (ME-1511-33194), the Clinical and Translational Science Award (UL1 TR001439) from the National Center for Advancing Translational Sciences at the National Institutes of Health, and by the National Library of Medicine (R01 LM012095) at the National Institutes of Health. The content is solely the responsibility of the authors, and does not necessarily represent the official views of the Patient-Centered Outcomes Research Institute, or the National Institutes of Health. The Medicare data were analyzed using a CMS data-use agreement (CMS DUA RSCH-2017-51404).

## REFERENCES

1. McClellan J, King M-C. Genetic Heterogeneity in Human Disease. *Cell*. 141(2):210-7. doi: 10.1016/j.cell.2010.03.032.
2. Waldman SA, Terzic A. Therapeutic targeting: a crucible for individualized medicine. *Clinical Pharmacology & Therapeutics*. 2008;83(5):651-4.
3. Rouzier R, Perou CM, Symmans WF, Ibrahim N, Cristofanilli M, Anderson K, et al. Breast cancer molecular subtypes respond differently to preoperative chemotherapy. *Clinical cancer research: an official journal of the American Association for Cancer Research*. 2005;11(16):5678-85. Epub 2005/08/24. doi: 10.1158/1078-0432.ccr-04-2421. PubMed PMID: 16115903.
4. Sorlie T, Perou CM, Tibshirani R, Aas T, Geisler S, Johnsen H, et al. Gene expression patterns of breast carcinomas distinguish tumor subclasses with clinical implications. *Proceedings of the National Academy of Sciences of the United States of America*. 2001;98(19):10869-74. Epub 2001/09/13. doi: 10.1073/pnas.191367098. PubMed PMID: 11553815; PubMed Central PMCID: PMC158566.
5. Fitzpatrick AM, Teague WG, Meyers DA, Peters SP, Li X, Li H, et al. Heterogeneity of severe asthma in childhood: confirmation by cluster analysis of children in the National Institutes of Health/National Heart, Lung, and Blood Institute Severe Asthma Research Program. *The Journal of allergy and clinical immunology*. 2011;127(2):382-9.e1-13. Epub 2011/01/05. doi: 10.1016/j.jaci.2010.11.015. PubMed PMID: 21195471; PubMed Central PMCID: PMC3060668.
6. Halder P, Pavord ID, Shaw DE, Berry MA, Thomas M, Brightling CE, et al. Cluster analysis and clinical asthma phenotypes. *American journal of respiratory and critical care medicine*. 2008;178(3):218-24. Epub 2008/05/16. doi: 10.1164/rccm.200711-1754OC. PubMed PMID: 18480428; PubMed Central PMCID: PMC158566.
7. Lotvall J, Akdis CA, Bacharier LB, Bjermer L, Casale TB, Custovic A, et al. Asthma endotypes: a new approach to classification of disease entities within the asthma syndrome. *The Journal of allergy and clinical immunology*. 2011;127(2):355-60. Epub 2011/02/02. doi: 10.1016/j.jaci.2010.11.037. PubMed PMID: 21281866.
8. Nair P, Pizzichini MMM, Kjarsgaard M, Inman MD, Efthimiadis A, Pizzichini E, et al. Mepolizumab for Prednisone-Dependent Asthma with Sputum Eosinophilia. *New England Journal of Medicine*. 2009;360(10):985-93. doi: 10.1056/NEJMoa0805435. PubMed PMID: 19264687.
9. Ortega HG, Liu MC, Pavord ID, Brusselle GG, FitzGerald JM, Chetta A, et al. Mepolizumab Treatment in Patients with Severe Eosinophilic Asthma. *New England Journal of Medicine*. 2014;371(13):1198-207. doi: 10.1056/NEJMoa1403290.
10. Collins FS, Varmus H. A new initiative on precision medicine. *The New England journal of medicine*. 2015;372(9):793-5. Epub 2015/01/31. doi: 10.1056/NEJMp1500523. PubMed PMID: 25635347.
11. Bhavnani SK, Kummerfeld E, Zhang W, Kuo Y-F, Garg N, Visweswaran S, et al. Heterogeneity in COVID-19 Patients at Multiple Levels of Granularity: From Biclusters to Clinical Interventions. *Proceedings of the American Medical Informatics Association Summits*. 2021:112-21. doi: PMID: 34457125.
12. Lacy ME, Wellenius GA, Carnethon MR, Loucks EB, Carson AP, Luo X, et al. Racial Differences in the Performance of Existing Risk Prediction Models for Incident Type 2 Diabetes: The CARDIA Study. *Diabetes care*. 2015. Epub 2015/12/03. doi: 10.2337/dc15-0509. PubMed PMID: 26628420.
13. Baker JJ. Medicare payment system for hospital inpatients: diagnosis-related groups. *Journal of health care finance*. 2002;28(3):1-13. Epub 2002/06/25. PubMed PMID: 12079147.
14. Lipkovich I, Dmitrienko A, Denne J, Enas G. Subgroup identification based on differential effect search--a recursive partitioning method for establishing response to treatment in patient subpopulations. *Statistics in medicine*. 2011;30(21):2601-21. Epub 2011/07/26. doi: 10.1002/sim.4289. PubMed PMID: 21786278.
15. Kehl V, Ulm K. Responder identification in clinical trials with censored data. *Comput Stat Data Anal*. 2006;50(5):1338-55. doi: 10.1016/j.csda.2004.11.015.
16. Hastie T, Tibshirani R, Friedman J. *The Elements of Statistical Learning*. New York, NY, USA: Springer New York Inc.; 2001.
17. Abu-jamous B, Fa R, Nandi AK. *Integrative Cluster Analysis in Bioinformatics*. Chichester, West Sussex, United Kingdom: John Wiley & Sons, Ltd.; 2015.

18. Lochner KA, Cox CS. Prevalence of multiple chronic conditions among Medicare beneficiaries, United States, 2010. Preventing chronic disease. 2013;10:E61. Epub 2013/04/27. doi: 10.5888/pcd10.120137. PubMed PMID: 23618541; PubMed Central PMCID: PMCPCmc3652723.
19. Aryal S, Diaz-Guzman E, Mannino DM. Prevalence of COPD and comorbidity. European Respiratory Monograph. 2013;59:1-12.
20. Baty F, Putora PM, Isenring B, Blum T, Brutsche M. Comorbidities and burden of COPD: a population based case-control study. PloS one. 2013;8(5):e63285. Epub 2013/05/22. doi: 10.1371/journal.pone.0063285. PubMed PMID: 23691009; PubMed Central PMCID: PMCPCmc3656944.
21. Moni MA, Lio P. Network-based analysis of comorbidities risk during an infection: SARS and HIV case studies. BMC bioinformatics. 2014;15:333. Epub 2014/10/26. doi: 10.1186/1471-2105-15-333. PubMed PMID: 25344230; PubMed Central PMCID: PMCPCmc4363349.
22. Cramer AO, Waldorp LJ, van der Maas HL, Borsboom D. Comorbidity: a network perspective. The Behavioral and brain sciences. 2010;33(2-3):137-50; discussion 50-93. Epub 2010/06/30. doi: 10.1017/s0140525x09991567. PubMed PMID: 20584369.
23. Islam MM, Valderas JM, Yen L, Dawda P, Jowsey T, McRae IS. Multimorbidity and comorbidity of chronic diseases among the senior Australians: prevalence and patterns. PloS one. 2014;9(1):e83783. Epub 2014/01/15. doi: 10.1371/journal.pone.0083783. PubMed PMID: 24421905; PubMed Central PMCID: PMCPCmc3885451.
24. Folino F, Pizzuti C, Ventura M. A comorbidity network approach to predict disease risk. Proceedings of the First international conference on Information technology in bio- and medical informatics; Bilbao, Spain. 1885260: Springer-Verlag; 2010. p. 102-9.
25. Newman MEJ. Networks: An Introduction. Oxford, United Kingdom: Oxford University Press; 2010.
26. Treviño S, Nyberg A, Del Genio CI, Bassler KE. Fast and accurate determination of modularity and its effect size. Journal of Statistical Mechanics: Theory and Experiment. 2015;2015(2):P02003. doi: 10.1088/1742-5468/2015/02/p02003.
27. Chauhan R, Ravi J, Datta P, Chen T, Schnappinger D, Bassler KE, et al. Reconstruction and topological characterization of the sigma factor regulatory network of Mycobacterium tuberculosis. Nature communications. 2016;7:11062. Epub 2016/04/01. doi: 10.1038/ncomms11062. PubMed PMID: 27029515; PubMed Central PMCID: PMCPCMC4821874.
28. Bhavnani SK, Dang B, Penton R, Visweswaran S, Bassler KE, Chen T, et al. How High-Risk Comorbidities Co-Occur in Readmitted Patients With Hip Fracture: Big Data Visual Analytical Approach. JMIR Med Inform. 2020;8(10):e13567. doi: 10.2196/13567.
29. Fruchterman T, Reingold E. Graph Drawing by Force-Directed Placement. Software – Practice & Experience. 1991;21(11):1129–64.
30. Dang B, Chen T, Bassler KE, Bhavnani SK. ExplodeLayout: Enhancing the Comprehension of Large and Dense Networks. AMIA Jt Summits Transl Sci Proc 2016.
31. Bhavnani SK, Chen T, Ayyaswamy A, Visweswaran S, Bellala G, Rohit D, et al. Enabling Comprehension of Patient Subgroups and Characteristics in Large Bipartite Networks: Implications for Precision Medicine. Proceedings of AMIA Joint Summits on Translational Science. 2017:21-9. Epub 2017/08/18. PubMed PMID: 28815099; PubMed Central PMCID: PMCPCMC5543384.
32. Bhavnani SK, Eichinger F, Martini S, Saxman P, Jagadish HV, Kretzler M. Network analysis of genes regulated in renal diseases: implications for a molecular-based classification. BMC bioinformatics. 2009;10 Suppl 9:S3. Epub 2009/09/26. doi: 10.1186/1471-2105-10-s9-s3. PubMed PMID: 19761573; PubMed Central PMCID: PMCPCMC2745690.
33. Bhavnani SK, Bellala G, Ganesan A, Krishna R, Saxman P, Scott C, et al. The nested structure of cancer symptoms. Implications for analyzing co-occurrence and managing symptoms. Methods of information in medicine. 2010;49(6):581-91. Epub 2010/11/19. doi: 10.3414/me09-01-0083. PubMed PMID: 21085743; PubMed Central PMCID: PMCPCMC3647463.
34. Bhavnani SK, Ganesan A, Hall T, Maslowski E, Eichinger F, Martini S, et al. Discovering hidden relationships between renal diseases and regulated genes through 3D network visualizations. BMC research notes. 2010;3:296. Epub 2010/11/13. doi: 10.1186/1756-0500-3-296. PubMed PMID: 21070623; PubMed Central PMCID: PMCPCMC3001742.

35. Bhavnani SK, Victor S, Calhoun WJ, Busse WW, Bleecker E, Castro M, et al. How cytokines co-occur across asthma patients: from bipartite network analysis to a molecular-based classification. *Journal of biomedical informatics*. 2011;44 Suppl 1:S24-30. Epub 2011/10/12. doi: 10.1016/j.jbi.2011.09.006. PubMed PMID: 21986291; PubMed Central PMCID: PMC3277832.
36. Bhavnani SK, Bellala G, Victor S, Bassler KE, Visweswaran S. The role of complementary bipartite visual analytical representations in the analysis of SNPs: a case study in ancestral informative markers. *Journal of the American Medical Informatics Association: JAMIA*. 2012;19(e1):e5-e12. Epub 2012/06/22. doi: 10.1136/amiainl-2011-000745. PubMed PMID: 22718038; PubMed Central PMCID: PMC3392853.
37. Bhavnani SK, Dang B, Bellala G, Divekar R, Visweswaran S, Brasier AR, et al. Unlocking proteomic heterogeneity in complex diseases through visual analytics. *Proteomics*. 2015;15(8):1405-18. Epub 2015/02/17. doi: 10.1002/pmic.201400451. PubMed PMID: 25684269; PubMed Central PMCID: PMC34471338.
38. Bhavnani SK, Dang B, Kilaru V, Caro M, Visweswaran S, Saade G, et al. Methylation differences reveal heterogeneity in preterm pathophysiology: results from bipartite network analyses. *Journal of perinatal medicine*. 2018;46(5):509-21. Epub 2017/07/01. doi: 10.1515/jpm-2017-0126. PubMed PMID: 28665803; PubMed Central PMCID: PMC5971156.
39. Jencks SF, Williams MV, Coleman EA. Rehospitalizations among Patients in the Medicare Fee-for-Service Program. *N Engl J Med*. 2009;360(14):1418-28. doi: doi:10.1056/NEJMs0803563. PubMed PMID: 19339721.
40. Report to Congress: Promoting Greater Efficiency in Medicare. Washington D.C.: MedPac (Medical Payment Advisory Commission); 2007.
41. Ashton CM, Del Junco DJ, Soucek J, Wray NP, Mansur CL. The association between the quality of inpatient care and early readmission: a meta-analysis of the evidence. *Medical care*. 1997;35(10):1044-59. Epub 1997/10/24. PubMed PMID: 9338530.
42. Yale New Haven Health Services Corporation/Center for Outcomes Research & Evaluation. 2015 Condition-specific measures updates and specifications report: Hospital-level 30-day risk-standardized readmission measures on acute myocardial infarction, heart failure, pneumonia, chronic obstructive pulmonary disease, and stroke. A report prepared for the Centers for Medicare & Medicaid Services (CMS) 2015 [April 20, 2015]. Available from: <http://www.cms.gov/Medicare/Quality-Initiatives-Patient-Assessment-Instruments/HospitalQualityInits/Measure-Methodology.html>.
43. Keenan PS, Normand SL, Lin Z, Drye EE, Bhat KR, Ross JS, et al. An administrative claims measure suitable for profiling hospital performance on the basis of 30-day all-cause readmission rates among patients with heart failure. *Circ Cardiovasc Qual Outcomes*. 2008;1(1):29-37. Epub 2008/09/01. doi: 10.1161/circoutcomes.108.802686. PubMed PMID: 20031785.
44. Yale New Haven Health Services Corporation/Center for Outcomes Research & Evaluation. 2015 Procedure-specific readmission measures updates and specifications report: Elective primary total hip arthroplasty and/or total knee arthroplasty, and isolated coronary artery bypass graft surgery. A report prepared for the Centers for Medicare & Medicaid Services (CMS) 2015 [April 20, 2015]. Available from: <http://www.cms.gov/Medicare/Quality-Initiatives-Patient-Assessment-Instruments/HospitalQualityInits/Measure-Methodology.html>.
45. Lochner KA, Cox CS. Prevalence of Multiple Chronic Conditions Among Medicare Beneficiaries, United States, 2010. *Prev Chronic Dis*. 2013;10:E61. doi: 10.5888/pcd10.120137.
46. Sharif R, Parekh TM, Pierson KS, Kuo YF, Sharma G. Predictors of early readmission among patients 40 to 64 years of age hospitalized for chronic obstructive pulmonary disease. *Ann Am Thorac Soc*. 2014;11(5):685-94. Epub 2014/05/03. doi: 10.1513/AnnalsATS.201310-358OC. PubMed PMID: 24784958; PubMed Central PMCID: PMC34225809.
47. Grosso LM, Curtis JP, Lin Z, Geary LL, Vellanki S, Oladele C, et al. Hospital-level 30-Day All-Cause Risk-Standardized Readmission Rate Following Elective Primary Total Hip Arthroplasty (THA) And/Or Total Knee Arthroplasty (TKA). Yale New Haven Health Services Corporation/Center for Outcomes Research & Evaluation, 2012.

48. Charlson ME, Pompei P, Ales KL, MacKenzie CR. A new method of classifying prognostic comorbidity in longitudinal studies: development and validation. *J Chronic Dis.* 1987;40(5):373-83. PubMed PMID: 3558716.
49. Elixhauser A, Steiner C, Harris DR, Coffey RM. Comorbidity measures for use with administrative data. *Medical care.* 1998;36(1):8-27. PubMed PMID: 9431328.
50. Yale New Haven Health Services Corporation/Center for Outcomes Research & Evaluation. 2017 Condition-specific measures updates and specifications report: Hospital-level 30-day risk-standardized readmission measures on acute myocardial infarction, heart failure, pneumonia, chronic obstructive pulmonary disease, and stroke. A report prepared for the Centers for Medicare & Medicaid Services (CMS) 2017 [June 1, 2017]. Available from: <https://www.cms.gov/Medicare/Quality-Initiatives-Patient-Assessment-Instruments/HospitalQualityInits/Measure-Methodology.html>.
51. SAS. Using SAS® to Perform Individual Matching in Design of Case-Control Studies 2010 [cited 2020 May, 5th]. Available from: <https://support.sas.com/resources/papers/proceedings10/061-2010.pdf>.
52. Rand WM. Objective Criteria for the Evaluation of Clustering Methods. *Journal of the American Statistical Association.* 1971;66(336):846-50. doi: 10.2307/2284239.
53. Bennett TD, Moffitt RA, Hajagos JG, Amor B, Anand A, Bissell MM, et al. The National COVID Cohort Collaborative: Clinical Characterization and Early Severity Prediction. *medRxiv.* 2021. Epub 2021/01/21. doi: 10.1101/2021.01.12.21249511. PubMed PMID: 33469592; PubMed Central PMCID: PMC7814838  
Amin Manna, and Nabeel Qureshi: employee of Palantir Technologies; Brian T. Garibaldi: Member of the FDA Pulmonary-Allergy Drugs Advisory Committee (PADAC); Matvey B. Palchuk: employee of TriNetX; Kristin Kostka: employee of IQVIA Inc.; Julie A. McMurry: and Melissa A. Haendel Cofounders of Pryzm Health; Chris P. Austin and Ken R. Gersing, employees of the National Institutes of Health. No conflicts of interest reported for all other authors.
54. Topaloglu U, Palchuk MB. Using a Federated Network of Real-World Data to Optimize Clinical Trials Operations. *JCO clinical cancer informatics.* 2018;2:1-10. Epub 2019/01/18. doi: 10.1200/cci.17.00067. PubMed PMID: 30652541; PubMed Central PMCID: PMC6816049.
55. Dogrusoz U, Karacelik A, Safarli I, Balci H, Dervishi L, Siper MC. Efficient methods and readily customizable libraries for managing complexity of large networks. *PloS one.* 2018;13(5):e0197238. Epub 2018/05/31. doi: 10.1371/journal.pone.0197238. PubMed PMID: 29813080; PubMed Central PMCID: PMC5973603 the following competing interests: I.S., H.B., and L.D. were supported through Google Summer of Code for implementing some of the algorithms in this work as part of open source software projects. Others have no competing interests. This does not alter the authors' adherence to PLOS ONE policies on sharing data and materials.
56. Wu J, Zhu F, Liu X, Yu H. An Information-Theoretic Framework for Evaluating Edge Bundling Visualization. *Entropy (Basel, Switzerland).* 2018;20(9). Epub 2018/08/21. doi: 10.3390/e20090625. PubMed PMID: 33265714; PubMed Central PMCID: PMC7513140.
57. Dhillon IS, Sra S. Generalized nonnegative matrix approximations with Bregman divergences. *Proceedings of the 18th International Conference on Neural Information Processing Systems; Vancouver, British Columbia, Canada.* 2976284: MIT Press; 2005. p. 283-90.
58. Dilsizian ME, Siegel EL. Machine Meets Biology: a Primer on Artificial Intelligence in Cardiology and Cardiac Imaging. *Current cardiology reports.* 2018;20(12):139. Epub 2018/10/20. doi: 10.1007/s11886-018-1074-8. PubMed PMID: 30334108.
59. Bhavnani SK, Visweswaran S, Divekar R, Brasier AR. Towards Team-Centered Informatics: Accelerating Innovation in Multidisciplinary Scientific Teams Through Visual Analytics. *The Journal of Applied Behavioral Science.* 2018:0021886318794606. doi: 10.1177/0021886318794606.
60. Wooten KC, Calhoun WJ, Bhavnani S, Rose RM, Ameredes B, Brasier AR. Evolution of Multidisciplinary Translational Teams (MTTs): Insights for Accelerating Translational Innovations. *Clinical and translational science.* 2015;8(5):542-52. Epub 2015/03/25. doi: 10.1111/cts.12266. PubMed PMID: 25801998; PubMed Central PMCID: PMC4575623.

## APPENDIX-1

### Analytical Methods for the MIPS Framework

Model	Inputs	Outputs
<b>1. Visual Analytical Model</b> (Bipartite Network Analysis)	<ul style="list-style-type: none"> <li><b>Training Dataset:</b> 50% random sample of 100% cases, and an equal number of 1:1 matched controls (used only for feature selection)</li> <li><b>Replication Dataset:</b> 50% random sample of 100% cases and equal number of 1:1 matched controls</li> </ul>	<ul style="list-style-type: none"> <li><b>Model Training</b>  <u>Feature Selection:</u> Set of comorbidities univariably significant in both the training and replication datasets  <u>Biclustering:</u> Modularity (degree of biclusteredness) and its significance, number of biclusters (subgroups), and their patient and comorbidity members in the training and replication datasets </li> <li><b>Model Replication</b>  <u>Comorbidity Co-Occurrence:</u> Rand Index (degree of replication), and its significance to measure replicability of comorbidity co-occurrence </li> <li><b>Model Interpretation</b>  <u>Visualization:</u> Layout of the bipartite network juxtaposed with risk of individual comorbidities and subgroups  <u>Clinical Significance:</u> Interpretation by clinicians for face validity of patient subgroups based on comorbidity co-occurrence, leading to inference of mechanisms precipitating readmission, and interventions </li> </ul>
<b>2. Classification Model</b> (Multinomial Logistic Regression)	<ul style="list-style-type: none"> <li><b>Training Dataset:</b> Random sample of 75% cases, with bicluster membership</li> <li><b>Internal Validation Dataset:</b> Random sample of 25% of cases (with subgroup membership used to validate the model)</li> </ul>	<ul style="list-style-type: none"> <li><b>Model Training</b>  <u>Subgroup Membership:</u> Probability of membership of each case to each subgroup (soft labels), with the highest used to determine subgroup membership (hard labels) </li> <li><b>Model Internal Validation</b>  <u>Internal Validation:</u> Accuracy of classification model based on hard labels </li> <li><b>Model Application</b>  <u>Classification:</u> Subgroup classification of 100% cases and 100% controls  <u>Subgroup Risk:</u> Proportion of cases in each subgroup </li> </ul>
<b>3. Prediction Model</b> (Binary Logistic Regression, and Hierarchical Binary Logistic Regression)	<ul style="list-style-type: none"> <li><b>Training Dataset:</b> Random samples of 75% of 100% cases and controls, with subgroup membership</li> <li><b>Internal Validation Dataset:</b> Random sample of 25% of cases and controls (with case/control labels used to validate the model)</li> </ul>	<ul style="list-style-type: none"> <li><b>Model Training</b>  <u>Predicted Risk:</u> Each patient's probability of being readmitted. </li> <li><b>Model Internal Validation</b>  <u>Internal Validation:</u> C-statistic (discrimination), and calibration-in-the-large and calibration slope (calibration) </li> <li><b>Model Comparison</b>  <u>Accuracy:</u> Net Reclassification Improvement (NRI) and Integrated Discrimination Improvement (IDI) </li> </ul>

**Table 1.** Inputs used to train and replicate/validate the three models, and the analytical outputs they produced.

Visual Analytical Modeling. The data used to build the visual analytical model consisted of 100% cases, and an equal number of 1:1 matched controls extracted by randomly selecting a control without replacement to match each case based on age, gender, race/ethnicity, and Medicaid eligibility [1]. The resulting dataset was divided randomly into a training (50%) and replication (50%) dataset (we use the term *replication* to avoid confusion with the term *validation* typically used in classification and prediction models). We used a bipartite network to model the cases (30-day readmitted patients) and significant comorbidities in each index condition using the following steps:

A. *Model Training.* The training of the bicluster network model consisted of the following two steps:

- I. *Feature Selection.* Given the large number of patients and comorbidities in the dataset, we used feature selection to identify comorbidities with the strongest signal and therefore interpretability for readmission using the following steps: (1) excluded comorbidities with prevalence less than 1% (as is commonly done in studies to reduce noise [2]); (2) selected significant comorbidities in the training dataset based on a 2-way interaction test using odds ratio (OR) with directionality, and correcting for multiple testing using Bonferroni, and (3) tested the surviving comorbidities for replication in the replication dataset, and selected those that were significant in both datasets. Appendix-2 shows the number of comorbidities, and variables that were included in the analysis for each of the three index conditions. The above feature

selection generated a single set of significant and replicated comorbidities used for the following bipartite network analysis.

- II. *Biclustering*. We used bipartite networks analysis [3] on the training dataset to analyze heterogeneity in readmission using the following steps: (1) Removed all cases that did not have any comorbidities (as the modularity maximization algorithm will trivially put disconnected nodes into a separate cluster). (2) Represented the cases (30-day readmitted patients in the training dataset) and their significant and replicated comorbidities (selected in Step A) as a bipartite network. As shown in Fig. 1, the nodes represented cases (circles) or comorbidities (triangles), and edges (lines) represented which case had which comorbidity. (3) Used a bipartite modularity maximization algorithm [4-6], to identify the number of biclusters, their members, and degree of biclusteredness of the network using modularity. Modularity is defined as the fraction of edges falling within a cluster, minus the expected fraction of such edges in a network of the same size with randomly assigned edges. Modularity ranges from -0.5 to +1, with values >0 indicating biclustering that is higher than can be expected by chance. We used the bipartite version of modularity to find biclusters in the network. (4) Measured the significance of the bicluster modularity by comparing it to a distribution of the same quantity generated from 1000 random permutations of the network, by preserving the network size (number of nodes) and the network density (number of edges).

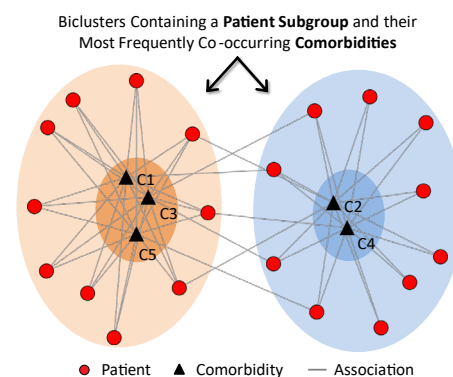


**Fig. 1.** A bipartite network showing patient subgroups and their most frequently co-occurring comorbidities.

- B. *Model Replication*. Repeated the above biclustering steps 1-4 to identify subgroups in the replication dataset, and compared the comorbidity co-occurrence in the training dataset, to that in the replication dataset using the Rand index (RI) [7]. RI measures the proportion of comorbidity pairs that co-occurred and did not co-occur in a cluster in the training and replication datasets (where 0=no inter-network cluster similarity, and 1=total inter-network cluster similarity). The significance of RI was measured by comparing it to a distribution of the same quantity generated from 1000 random permutations of the training and replication networks. All tests of statistical significance in Steps A and B were 2-sided.
- C. *Model Interpretation*. The model interpretation consisted of the following steps:
  - I. *Visualization*. We used the following steps to visualize the network generated from the training dataset. (1) Used *Fruchterman-Reingold* (FR) [8], a force-directed algorithm to lay out the bipartite network. This layout algorithm pulls together nodes that are strongly connected, and pushes apart nodes that are not. This results in nodes with a similar pattern of connections to be placed close to each other in Euclidean space, and those that are dissimilar are pushed apart. (2) As the FR algorithm often cannot entirely separate clusters in large and dense networks, the network layout needs to be visually enhanced before it is interpretable by clinician stakeholders. Therefore, we used the *ExplodeLayout* algorithm [9, 10] to separate the biclusters to reduce their visual overlap. This algorithm preserves the distances of nodes within a bicluster, but increases the distance of nodes between clusters to improve interpretability. (3) Juxtaposed the risk of readmission with the network visualization (in response to a request from the clinical stakeholders). This was done by (a) displaying comorbidity labels with their univariable ORs for readmission (measured in Step A) ranked by their odds ratios (ORs) for each subgroup, and (b) measuring the readmission risk for each patient subgroup based on the full case-control population (explained in more detail in the section on classification modeling), and juxtaposing it with the respective subgroup.
  - II. *Clinical Interpretation*. We used the following steps to solicit clinical interpretations of the above bipartite network. (1) Recruited a pulmonologist specializing in COPD and hospital readmission to interpret the COPD results, and a geriatrician with expertise in treating older adults in CHF and THA/TKA to interpret the respective results. (2) Requested each clinician stakeholder to interpret the patient subgroups, their mechanisms, and potential interventions to reduce the risk for readmission.

**Classification Modeling.** As shown in the bipartite network example in Fig. 1, the biclusters identified through the modularity maximization algorithm contain patient subgroups and their *most frequently* co-occurring comorbidities with respect to other patients in the network. However, there are often many edges between biclusters, revealing that many patients within a bicluster have comorbidities that exist in other biclusters. As is true for most partitioning cluster methods, including modularity, membership of a new patient to each bicluster is therefore *probabilistic*. The classification of a patient into a cluster is therefore not defined by the *inclusion or exclusion of comorbidities* (e.g., hypertension and diabetes), but rather by the *probability* of being in a patient subgroup. Patients are therefore similar or different, not just in a handful of carefully-selected comorbidities while ignoring others, but based on *all* of their recorded comorbidities. This overall profile of patients reflects the reality of comorbid conditions.

To model the above complexity, we used multinomial logistic regression [11] to develop classification models in each index condition. This approach has the advantage of generating probabilities (“soft labels”) for a patient to belong to each patient subgroup. The models were trained, internally validated, and then applied to generate information for the other two modeling methods, as described below:

- A. **Model Training.** The data used to build the classification model consisted of the training dataset and subgroup membership from the visual analytical model. We trained a multinomial logistic regression model using the above data, with independent variables that included comorbidities identified through feature selection done for the visual analytical modeling. Accuracy of the trained model was measured by calculating the percentage of times the model correctly classified the cases into the subgroups, using the highest predicted probability across the subgroups (“hard labels”).
- B. **Model Internal Validation.** To internally validate the classifier, we randomly split the above data into training (75%) and testing (25%) datasets, 1000 times. For each iteration, we trained a model using the training dataset, and measured its accuracy on the testing dataset. This was done by predicting the subgroup membership using the highest predicted probability among all the subgroups. The overall predicted accuracy was then estimated by calculating the mean accuracy across the 1000 models.
- C. **Model Application.** Using the 100% cases, in addition to the 100% controls from July 2013-August 2014 (representing the entire Medicare population of each index condition from those years), we generated the following two types of information for use in the other models. (1) Used the classifier trained in Step A above, to classify 100% cases and 100% controls into a subgroup. This information was used by the subsequent predictive modeling. (2) While the visual analytical model used the 1:1 matched controls for feature selection, this cohort did not represent the entire population. Therefore, to accurately measure the subgroup risk, we used the entire case-control population classified into the subgroups (as described in the above step), and measured the proportion of cases in each subgroup. Furthermore, as requested by the clinicians, we juxtaposed these subgroup risks next to the respective subgroups in the bipartite network visualization, to improve their interpretability.

**Predictive Modeling.** The data used to build the predictive models consisted of 100% cases and 100% controls, in addition to their subgroup membership generated from the above classification models. These data were randomly split into a training (75%) and validation (25%) dataset. The predictive models were trained, internally validated, and compared for predictive accuracy, as described below:

- A. **Model Training.** We used the training dataset to train a Standard Model (binary logistic regression without subgroup membership similar to the CMS models), and a Hierarchical Model (binary logistic regression with subgroup membership), with 30-day unplanned readmission (yes vs. no) as the outcome. Independent variables for both models included comorbidities identified through the feature selection in each index condition (see Appendix-2), and demographics. The Hierarchical Model additionally included subgroup membership.
- B. **Model Internal Validation.** We used the validation dataset to internally validate the models through the following two measures:

- I. Discrimination (model's ability to distinguish readmitted patients from those not readmitted) was measured using the C-statistic, which is identical to the area under the receiver operating characteristic (ROC) curve. Model discrimination was examined using box plots to show the average risk prediction for patients with and without readmission.
  - II. Calibration (model's agreement of the predicted probabilities with the observed risk) was measured using calibration-in-the-large, and calibration slope, which was examined through a calibration plot showing the proportion of patients actually admitted, versus deciles of predicted probability of having readmission. Good calibration is when calibration-in-the-large is close to zero, and the calibration slope is close to one. Since the large sample size overpowered the study, we did not measure the calibration based on statistical significance (e.g., *P* values of the Hosmer-Lemeshow and calibration indices).
- C. *Model Comparisons.* We used the chi-squared test to compare the C-statistic of the Standard Model to that of the Hierarchical Model. We also measured the C-statistic of the Standard Model applied to each subgroup separately. This enabled examination of how the Standard Model performed on patient subgroups to identify, for example, which subgroups underperformed when using the current Standard Model.

Because the above models used the feature selection step to select comorbidities for use as independent variables, they differed from those used in the published CMS models. Therefore, to perform a head-to-head comparison with the published CMS models, we additionally developed a logistic regression model using independent variables that were identical to the published CMS model (CMS Standard Model), which was compared to the same model that included subgroup membership (CMS Hierarchical Model). We used the chi-squared test to compare the C-statistic of the CMS Standard Model to that from the CMS Hierarchical Model, in addition to the following measures of model accuracy:

- I. Net Reclassification Improvement (NRI) measured the proportion of patients whose predicted probability of readmission improved with reference to actual readmission status. We used two NRI statistics: (a) categorical NRI, which predicted readmission probabilities divided into 10 sequential categories ranging from 0-1, with improvement requiring a shift between categories; and (b) continuous NRI which is based on the proportions of patients with any improved predicted probability of readmission, regardless of the size of that improvement.
- II. Integrated Discrimination Improvement (IDI) measured the difference in the average improvement in predicted risks between the CMS Standard Model and the CMS Hierarchical Model.

## APPENDIX-2

### Patient Inclusion and Exclusion Criteria

#### ICD-9 Codes for Selecting Index Conditions

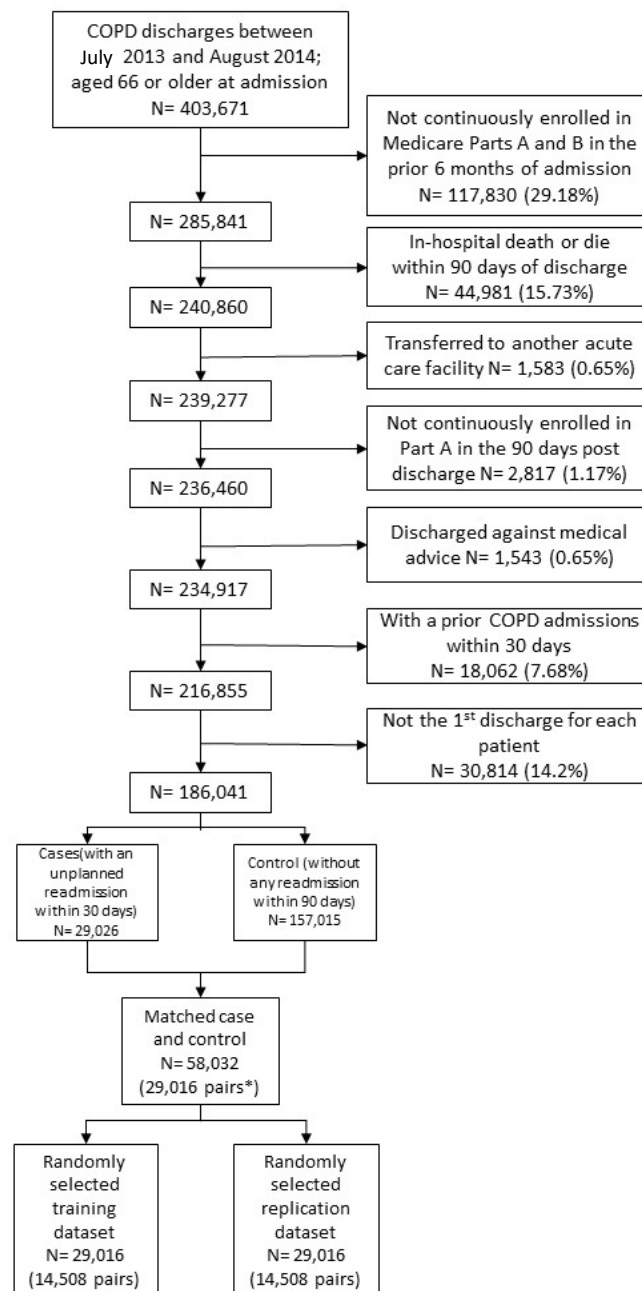
1. **Hospitalization for COPD** was defined as (1) hospitalization with a primary ICD-9 code for COPD (491.21, 491.22, 491.8, 491.9, 492.8, 493.20, 493.21, 493.22 and 496), or (2) primary ICD-9 codes of 518.81, 518.82, 518.84 or 799.1 and secondary ICD-9 codes for COPD (491.21, 491.22, 493.21 and 493.22).
2. **Hospitalization for CHF** was defined as hospitalization with a primary ICD-9 code for CHF (402.01, 402.01, 402.91, 404.01, 404.03, 404.11, 404.13, 404.91, 404.93 or 428.xx)
3. **Hospitalization for THA/TKA** was defined as hospitalization with a primary ICD-9 code for THA/TKA (81.51 and 81.54). We included admissions only for elective total hip/knee arthroplasty, and those with non-elective were excluded. These included admissions with a diagnosis of a femur, hip, or pelvic fracture, those who received partial hip arthroplasty, revision or resurfacing procedures concurrently with hip/knee arthroplasty, those with malignant bone neoplasm, or with a procedure code for removal of implanted devices/prostheses.

#### Inclusion and Exclusion Criteria

For each index condition, we used the same inclusion and exclusion criteria used to develop the CMS models, but with the most recent years (2013-2014) provided by Medicare when we started the project. We used 100% of the 30-day readmitted patients in 2013 and 2014 Medicare claims data, from which we extracted all patients that were admitted to an acute care hospital on or after July 2013-August 2014 with a principal diagnosis of the index condition, were 66 years of age or older, and were enrolled in both Medicare parts A and B fee-for-service plans in the 6 months before admission. Furthermore, we excluded patients who were transferred from other facilities, died during the hospitalization, or transferred to another acute care hospital. Similar to the CMS models, we selected the first admission for patients with multiple admissions during the study period, and did not use Medicare Part D (related to prescription medications).

Next, we extracted 100% controls who were not readmitted for at least 90 days since discharge. CMS uses this 90-day window of no re-admittance to ensure that the controls are substantially free of complications that result in readmission during this period [12, 13]. A small percentage (0.8%) of Medicare patients had “unknown race” for the Race attribute, so we grouped “unknown race” and “other race” and ensured that there was an equal number of them in the cases and control datasets. The low rate of missing data on race had too low a risk for bias to warrant a sensitivity analysis. The following flow charts describe the inclusion and exclusion criteria used to extract cases and controls for COPD, CHF, and THA/TKA, and the respective numbers of patients extracted at each step.

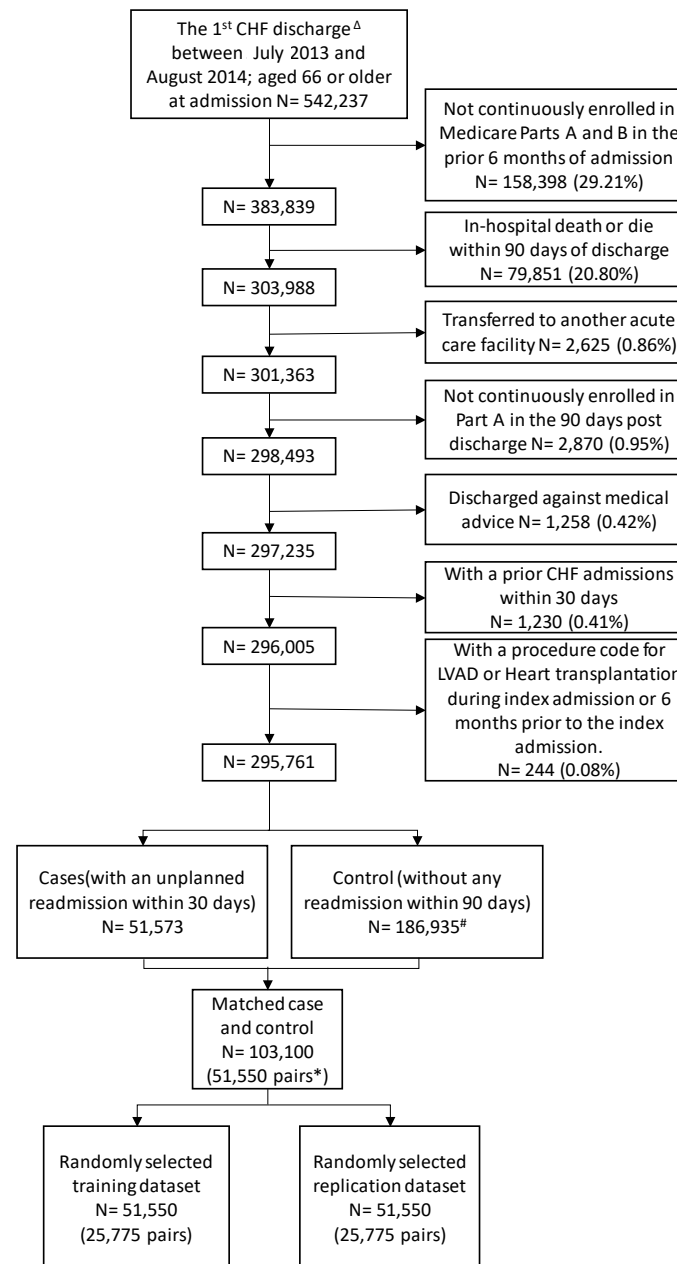
## Patient Inclusion and Exclusion Criteria for COPD Training and Replication Datasets



Cases and controls were matched on age, gender, race/ethnicity, and Medicaid eligibility

\*10 cases could not be matched

## Patient Inclusion and Exclusion Criteria for CHF Training and Replication Datasets

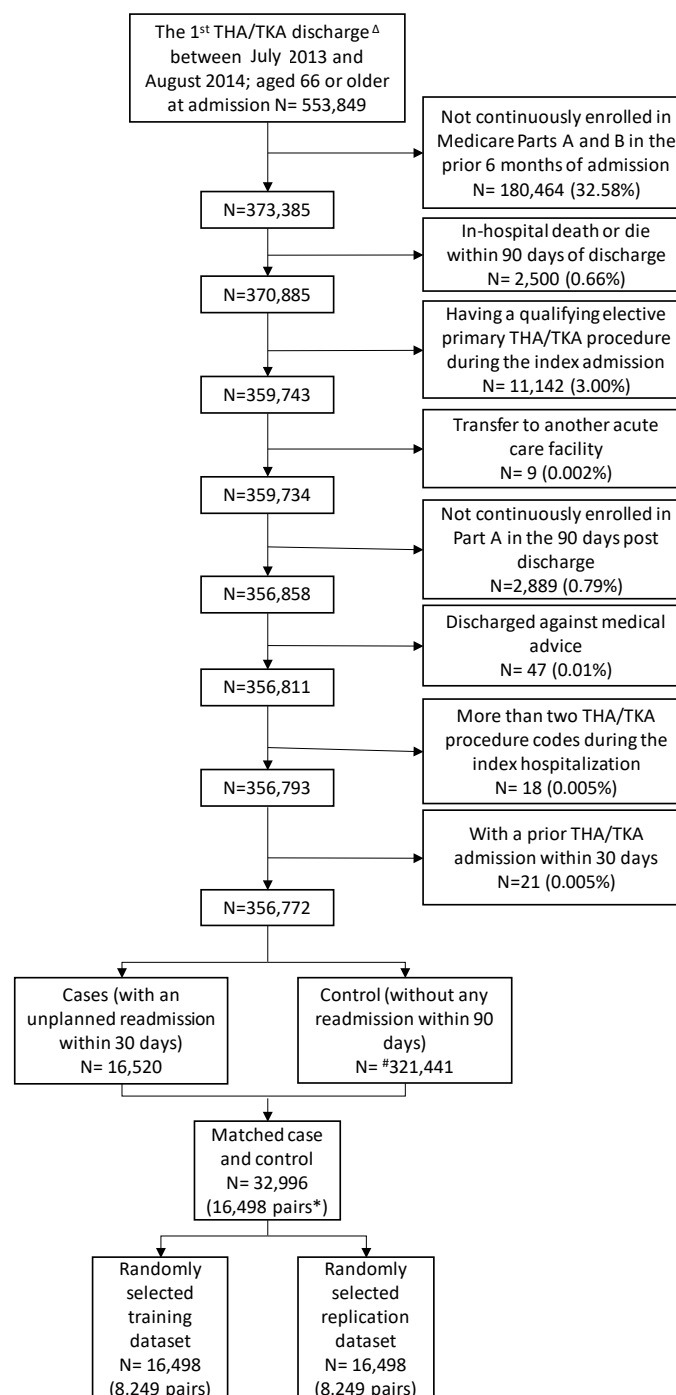


<sup>Δ</sup> When a patient had more than 1 CHF admission during this time period, only the first one was selected.

<sup>#</sup> 57,253 patients were readmitted within 90 days and therefore removed from the control pool.

\*Cases and controls were matched on age, gender, race/ethnicity, and Medicaid eligibility. There were 23 cases who could not be matched.

## Patient Inclusion and Exclusion Criteria for THA/TKA Training and Replication Datasets



<sup>Δ</sup> When a patient had more than 1 THA/TKA admission during this time period, only the first one was selected.

<sup>#</sup> 18,811 patients were readmitted within 90 days and therefore removed from the control pool.

\* Cases and controls were matched on age, gender, race/ethnicity, number of procedures, type of procedure (THA or TKA), and Medicaid eligibility. There were 22 cases who could not be matched.

## APPENDIX-3

### Variable and Feature Selection

#### COPD

The initial set of comorbidities included 45 comorbidities generated from a union of the three comorbidity indices, plus 2 condition-specific comorbidities recommended by the clinicians, resulting in 47 comorbidities. The following feature-selection steps resulted in 30 comorbidities surviving, that were used for the modeling:

1. Removed comorbidities with prevalence less than 1%, resulting in the following that were excluded, leaving 44 comorbidities:

Excluded Comorbidities	Label
1. RespDepend	Respirator dependence/respiratory failure (V22 CC 82-83)
2. Pancreatitis	Chronic pancreatitis (V22 CC 34)
3. HIV_AIDS	HIV/AIDS

2. Measured the OR of each comorbidity for readmission and excluded the following that were not significant (at the .05 level corrected for multiple testing with Bonferroni), leaving 40 comorbidities:

Excluded Comorbidities	Label
1. Neoplasm_other	Other digestive and urinary neoplasms (V22 CC 14)
2. Lymphatic	Lymphatic, head and neck, brain, and other major cancers; breast, colorectal and other cancers and tumors; other respiratory and heart neoplasms
3. Diabetes_wo_comp	Diabetes without complications
4. Rheumatic	Connective Tissue Disease-Rheumatic Disease

3. Conducted a two-way co-occurrence test resulting in none being excluded.
4. Conducted a two-way directionality test resulting in the following that were excluded:

Excluded Comorbidities	Label
1. Anxiety	Anxiety disorders (V22 CC 62)
2. Brain_disorder	Dementia or other specified brain disorders
3. Liver_disease	Liver disease
4. LungCa	Lung and other severe cancers (V22 CC 9)
5. Metastatic_cancer	Metastatic cancer or acute leukemia
6. Vertebral_fract	Vertebral fractures without spinal cord injury (V22 CC 169)

5. Repeated steps 2-4 in the replication dataset resulting in 30 comorbidities shown below:

Final Comorbidities	Label
1. Anemias	Iron deficiency or other/unspecified anemias and blood disease
2. Apnea	Sleep apnea
3. Arrhythmias	Specified arrhythmias and other heart rhythm disorders
4. CardioRespShock	Cardio-respiratory failure and shock (V22 CC 84)
5. Cellulitis	Cellulitis, local skin infection (V22 CC 164)

6. Coronary_angina	Coronary atherosclerosis or angina (V22 CC 88-89)
7. Coronary_syndrome	Acute coronary syndrome
8. Depression	Depression (V22 CC 61)
9. Diabetes_w_comp	Diabetes with complications
10. Endocrine_disorder	Endocrine and metabolic disorders; disorders of fluid/electrolyte/acidbase balance
11. GI_other	Other gastrointestinal disorders (V22 CC 38)
12. HD_other	Other and unspecified heart disease (V22 CC 98)
13. Heart_failure	Congestive heart failure
14. Hemiplegia	Hemiplegia, paraplegia, paralysis, functional disability
15. Hypertension_comp	Hypertension complicated
16. Hypertension_Uncomp	Hypertension uncomplicated
17. Infection	Severe infection; other infectious diseases (V22 CC 3-7)
18. Malnutrition	Protein-calorie malnutrition / weight loss
19. Morbid_OB	Morbid obesity; other endocrine/metabolic/nutritional disorders
20. MV	History of mechanical ventilation
21. Neurological_Disorders	Other Neurological Disorders
22. Neuropathy	Polyneuropathy / other neuropathies (V22 CC 75,81)
23. Peptic_ulcer	Peptic ulcer, hemorrhage, other specified gastrointestinal disorders
24. Pneu	Pneumonia (V22 CC 114-116)
25. psych_other	Other psychiatric disorders (V22 CC 63)
26. Psychosis	Drug/alcohol psychosis or dependence
27. Renal_failure	Renal failure
28. Ulcer	Decubitus ulcer or chronic skin ulcer (V22 CC 157-161)
29. Valvular_Disease	Valvular Disease
30. Vascular	Vascular or circulatory disease

## CHF

The initial set of comorbidities included 42 comorbidities generated from a union of the three comorbidity indices, plus 1 condition-specific comorbidities recommended by the clinicians, resulting in 43 comorbidities. The following feature-selection steps resulted in 37 comorbidities, that were used for the modeling:

1. Removed comorbidities with prevalence less than 1%, resulting in the following that were excluded, leaving 42 comorbidities:

Excluded Comorbidities	Label
1. HIV_AIDS	HIV/AIDS

2. Measured the OR of each comorbidity for readmission and excluded the following that were not significant (at the .05 level corrected for multiple testing with Bonferroni), leaving 40 comorbidities that had significant associations with readmission:

Excluded Comorbidities	Label
1. Metastatic_cancer	Metastatic cancer or acute leukemia
2. Diabetes_wo_comp	Diabetes Mellitus without Complication

3. Conducted a two-way co-occurrence test resulting in none being excluded.

4. Conducted a two-way directionality test, resulting in the following that were excluded leaving 39 variables that were involved in one or more significant direction tests:

Excluded Comorbidities	Label
1. Rheumatic	Rheumatic Disease

5. Repeated steps 2-4 in the replication dataset resulting in 37 comorbidities shown below:

Final Comorbidities	Label
1. Coronary_angina	Coronary atherosclerosis or angina (CC 88-89)
2. CABG	History of coronary artery bypass graft (CABG) surgery
3. COPD	Chronic Obstructive Pulmonary Disease (CC 111)
4. CardioRespShock	Cardio-respiratory failure and shock
5. Depression	Depression (CC 61)
6. Dialysis	Dialysis status (CC 134)
7. GI_other	Other gastrointestinal disorders (CC 38)
8. Hypertension_Comp	Hypertension Complicated
9. Hypertension_Uncomp	Hypertension Uncomplicated
10. Hypothyroidism	Hypothyroidism
11. Nephritis	Nephritis (CC 141)
12. Obesity	Obesity
13. Neuro_disorders	Other Neurological Disorders
14. HD_other	Other and unspecified heart disease (CC 98)
15. Psych_other	Other psychiatric disorders (CC 63)
16. Urinary_tract_disorder	Other urinary tract disorders (CC 145)
17. Pneu	Pneumonia (CC 114-116)
18. Renal_failure	Renal failure (CC 135-140)
19. Ulcer	Decubitus ulcer or chronic skin ulcer (CC 157-161)
20. Coronary_syndrome	Acute coronary syndrome
21. Psychosis	Drug/alcohol abuse/dependence/psychosis
22. Anemias	Iron deficiency or other/unspecified anemias and blood disease
23. Arrhythmia	Specified arrhythmias and other heart rhythm disorders
24. CHF	Congestive heart failure
25. Cancer	Cancer
26. Stroke	Stroke
27. Brain_disorders	Dementia or other specified brain disorders
28. Diabetes_w_comp	Diabetes Mellitus Complicated
29. Endocrine_disorders	Other significant endocrine and metabolic disorders; disorders of fluid/electrolyte/acid base balance
30. Liver_disease	Liver or biliary disease
31. Malnutrition	Protein-calorie malnutrition
32. Hemiplegia	Hemiplegia, paraplegia, paralysis, functional disability
33. Peptic_ulcer	Peptic ulcer, hemorrhage, other specified gastrointestinal disorders
34. Vascular	Vascular or circulatory disease
35. Psychiatric_disorders	Major psychiatric disorders
36. Hematological	Severe hematological disorders
37. Valvular_disease	Valvular and Rheumatic Heart Disease

## TKA/THA

The initial set of comorbidities included 39 comorbidities generated from a union of the three comorbidity indices, plus 2 condition-specific comorbidities recommended by the clinicians, resulting in 41 comorbidities. The following feature-selection steps resulted in 11 comorbidities, that were used for the modeling:

1. Removed comorbidities with prevalence less than 1%, resulting in the following that were excluded, leaving 30 comorbidities:

Excluded Comorbidities	Label
1. Other_Hip_Cong_Def	Other congenital deformity of hip (joint)
2. Post_Trau_Osteoarthritis	Post traumatic osteoarthritis
3. Dialysis_status	Dialysis status (CC 134)
4. Blood_Loss_Anemia	Blood Loss Anemia
5. Alcohol_Abuse	Alcohol Abuse
6. Drug_Abuse	Drug Abuse
7. HIV_AIDS	HIV/AIDS
8. Metastatic_cancer	Metastatic cancer or acute leukemia
9. Hemiplegia	Hemiplegia, paraplegia, paralysis, functional disability
10. Liver_disease	Liver disease
11. Peptic_ulcer	Peptic Ulcer Disease

2. Measured the OR of each comorbidity for readmission (at the .05 level corrected for multiple testing with Bonferroni), leaving all 30 comorbidities that had significant associations with readmission
3. Conducted a two-way co-occurrence test resulting in none being excluded.
4. Conducted a two-way directionality test, resulting in the following that were excluded leaving 19 variables that were involved in one or more significant direction tests:

Excluded Comorbidities	Label
1. Brain_disorders	Dementia or other specified brain disorders
2. Cancer	Cancer
3. Cellulitis	Cellulitis, local skin infection (CC 164)
4. Deficiency_Anemia	Deficiency Anemia
5. Diab_wo_comp	Diabetes mellitus
6. Hematological	Severe hematological disorders
7. Malnutrition	Protein-calorie malnutrition
8. Neuro_disorders	Other Neurological Disorders
9. Stroke	Stroke
10. Ulcer	Decubitus ulcer or chronic skin ulcer (CC 157-161)
11. Valvular_disease	Valvular Disease

5. Repeated steps 2 through 4 in the replicate dataset resulting in 11 comorbidities shown below:

Final Comorbidities	Label
1. Arrhythmia	Specified arrhythmias and other heart rhythm disorders
2. CHF	Congestive heart failure
3. COPD	Chronic Obstructive Pulmonary Disease
4. Coronary_angina	Coronary atherosclerosis or angina

5. Endocrine_disorders	Other significant endocrine and metabolic disorders; disorders of fluid/electrolyte/acidbase balance
6. Hypertension_Comp	Hypertension complicated
7. Hypertension_Uncomp	Hypertension Uncomplicated
8. Major_Symp_Abnormalities	Major symptoms, abnormalities (CC 178)
9. Morbid_OB	Morbidity obesity
10. Psychiatric_disorders	Major psychiatric disorders
11. Renal_failure	Renal failure (CC 135-140)

## APPENDIX-4

### Classification Modeling

#### Multinomial Logistic Regression Coefficients

##### **COPD**

	<b>Bicluster-2</b>	<b>Bicluster-3</b>	<b>Bicluster-4</b>
(Intercept)	9.478442033	-15.60229477	-20.58911845
MV	15.37003888	31.79526753	174.7625575
Apnea	14.73866236	30.13129952	174.8192981
Infection	13.07141525	30.94167533	175.7976241
GI_other	-138.0330506	-122.1606071	-141.8251611
Depression	11.44920157	194.57748	15.50399067
Psych_other	6.633772193	193.1120262	15.01395622
Neuropathy	4.22511563	191.7033722	11.82453364
CardioRespShock	15.935738	30.78720915	177.4810561
Coronary_angina	-140.3504037	-121.6295958	-139.1018879
HD_other	12.65500876	22.79910161	173.1189166
Pneu	12.40491598	192.8944261	14.40776138
Ulcer	25.40389722	36.65033091	174.4945337
Cellulitis	10.19338572	25.35264195	174.1779677
Valvular_Disease	179.470279	29.79933499	12.07687072
Hypertension_Uncomp	-144.0822947	-135.252917	-149.1763872
Hypertension_comp	169.9103199	9.909139715	-15.01176101
Neurological_Disorders	11.98793007	27.3962048	174.152075
Diabetes_w_comp	179.9458627	32.79407674	10.94569788
Malnutrition	2.619696434	190.2553747	10.57634814
Morbid_OB	-144.7853066	-126.4723011	-150.75158
Endocrine_disorder	18.25087715	30.17692505	173.8734803
Peptic_ulcer	14.57401571	33.3138924	174.6959617
Anemias	180.37182	32.01649034	11.85268168
Psychosis	0.808153461	190.136092	8.470673123
Hemiplegia	22.05837142	36.91425527	173.7515174
Heart_failure	179.4801884	29.61286201	6.090102717
Coronary_syndrome	17.65746601	31.18056088	177.0738381
Arrhythmias	-140.5676174	-122.0347651	-139.1832525
Vascular	12.82066036	29.47640378	174.8331118
Renal_failure	181.4635165	35.07327525	9.594086268

## CHF

	Bicluster-2	Bicluster-3	Bicluster-4
(Intercept)	4.228411649	3.221587055	4.404809652
CABG	-16.88332455	-16.46705046	-16.90410559
GI_other	1.608383181	18.42437593	2.537152385
Depression	1.744237257	18.57833534	2.132954431
Psych_other	1.565344584	18.89075678	1.851558983
CardioRespShock	1.899086259	2.614460813	20.82096349
Coronary_angina	-16.52943558	-16.50069914	-16.28824682
HD_other	1.630347764	1.900983651	20.69135601
COPD	2.208517874	18.8515632	2.812111665
Pneu	1.368125374	1.230710494	20.35722646
Dialysis_status	21.64550697	7.573268069	6.356824836
Renal_failure	16.64635654	3.207105993	2.875810167
Nephritis	24.05426922	11.91409993	8.430710694
Other_uri_tract_disorders	17.28359996	3.468138309	2.68316497
Ulcer	18.62035155	4.612512833	4.621717632
Hypertension_Uncomp	-16.17798732	-17.43341906	-17.17899564
Hypertension_Comp	18.21349274	2.666169079	2.719974312
Neuro_Disorders	3.174148638	3.426243554	21.7581539
Hypothyroidism	1.532038616	18.6465425	2.742755582
Obesity	16.77179346	3.477665718	1.851913596
Cancer	1.825845108	18.78533294	2.280566193
Diabetes_w_comp	16.97604199	3.131645807	2.25066864
Malnutrition	1.654276729	2.26075743	20.16266194
Endocrine_disorder	16.95913583	3.414523477	2.762293049
Liver_disease	0.509273487	1.346254075	19.37619302
Peptic_ulcer	1.882489155	2.868064904	20.99453939
Hematological	1.215479083	1.623296079	20.18186306
Anemias	16.84448889	2.650113464	2.132489404
Brain_disorders	1.214570676	19.0044895	2.119832832
Psychosis	1.612149611	18.59666356	2.038965354
Psychiatric_disorders	3.533134983	19.8653935	3.164125739
Hemiplegia	2.634196819	3.196095963	21.40555332
CHF	-16.83591928	-17.14949663	-16.56386079
Coronary_syndrome	1.423033472	2.813198347	20.7510375
Valvular_disease	-16.84402957	-16.55559304	-16.67291059
Arrhythmia	-17.41765184	-17.22878444	-17.44203684
Stroke	1.248759632	1.486455436	19.78749343
Vascular	0.908845182	1.356092137	19.93213936

## TKA/THA

	Bicluster-2	Bicluster-3	Bicluster-4	Bicluster-5	Bicluster-6	Bicluster-7
(Intercept)	-645.18	19.65	-365.25	-1.65	154.42	162.00
Renal_failure	568.98	529.82	1385.51	811.46	748.18	514.28
Major_Symp_Abnormalities	338.07	756.45	494.57	542.41	548.90	529.61
Hypertension_Uncomp	-863.03	-675.02	-695.36	-655.72	-711.68	-668.86
Hypertension_Comp	-380.60	-814.06	468.07	-52.64	-121.56	-260.13
Morbid_OB	229.35	294.47	409.00	492.63	824.96	492.19
Endocrine_disorders	426.79	310.04	1280.41	702.34	612.09	439.19
Psychiatric_disorders	-12.78	22.00	196.72	-634.96	-258.19	944.17
CHF	881.66	179.53	67.03	-113.47	-132.62	46.56
Coronary_angina	865.33	94.72	1.15	-184.54	-119.69	-108.41
Arrhythmia	936.49	95.61	77.56	-126.56	-133.83	-163.73
COPD	360.05	240.86	508.18	990.19	358.05	655.49

## Subgroup Risk

**COPD.** The COPD dataset included 186041 total patients, of which 29026 were cases (15.6%). The following are the percentage of cases in each bicluster (subgroup risk) after classification of the 100% cases and 100% controls by the classification model, and then juxtaposed with the visualization of the respective patient subgroups:

Bicluster	Total Patients	Cases	Percent	CI95 (Min)	CI95 (Max)
1	76296	9673	12.7%	12.4	12.9
2	43477	7731	17.8%	17.4	18.1
3	37174	5906	15.9%	15.5	16.3
4	29094	5716	19.6%	19.2	20.1

**CHF.** The CHF dataset included 295761 total patients, of which 51573 were cases (17.4%). The following are the percentage of cases in each bicluster (subgroup risk) after classification of the 100% cases and 100% controls into subgroups by the classification model, and juxtaposed with the visualization of the respective patient subgroups:

Bicluster	Total Patients	Cases	Percent	CI95 (Min)	CI95 (Max)
1	9673	76296	12.7%	12.4	12.9
2	7731	43477	17.8%	17.4	18.1
3	5906	37174	15.9%	15.5	16.3
4	5716	29094	19.6%	19.2	20.1

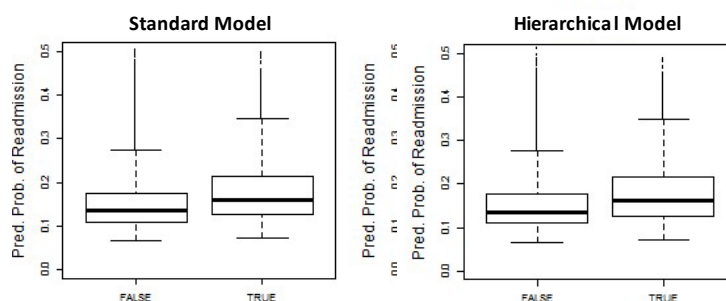
**THA/TKA.** The TKA/THA dataset included 356772 total patients, of which 16520 were cases (4.6%). The following are the percentage of cases in each bicluster (subgroup risk) after classification of 100% cases and 100% controls by the classification model, and then juxtaposed with the visualization of the respective patient subgroups:

Bicluster	Total Patients	Cases	Percent	CI95 (Min)	CI95 (Max)
1	2157	57045	3.8%	3.6	3.9
2	2317	33535	6.9%	6.6	7.2
3	2255	55260	4.1%	3.9	4.2
4	2135	29475	7.2%	7	7.5
5	2003	30856	6.5%	6.2	6.8
6	1945	43185	4.5%	4.3	4.7
7	3708	107416	3.5%	3.3	3.6

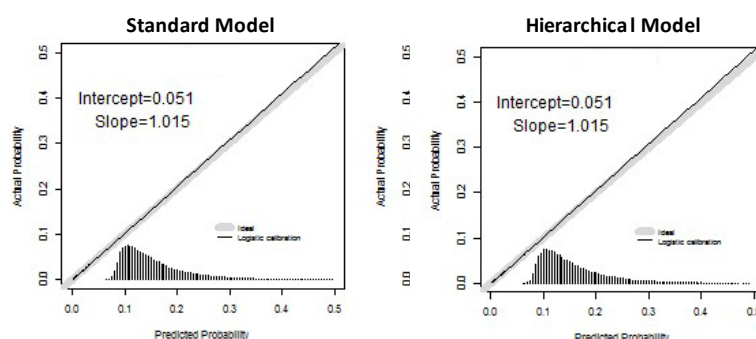
## APPENDIX-5 Predictive Modeling

### COPD

**Discrimination.** The following are box plots of risk prediction by readmission status for the Standard Model and the Hierarchical Model.



**Calibration.** The following are calibration plots showing logistic regressions relating readmission status to the logistic quantile of the predicted probability of readmission yield regression lines with specified intercept and slope (the ideal regression line would have intercept=0 and slope=1, which is shown shaded for reference). The histograms at the bottom of each graph reflect the frequency of modeled data, horizontal axes show predicted probability, vertical axes show actual probability, and the axes of all figures are constrained to range from 0 to .5.



**Coefficients.** Logistic regression coefficients relating readmission status to the logistic quantile of the predicted probability of readmission for each model, with standard errors.

	Intercept (Standard Error)	Slope (Standard Error)
Standard Model	0.051 (0.049)	1.015 (0.029)
Hierarchical Model	0.051 (0.049)	1.015 (0.029)

### Model Coefficients for Standard Model (COPD)

(Intercept)	-2.136379215
sex2	-0.018974047
AgeAdm	-0.006994626
RACE51	0.295066886
RACE52	0.341204445
RACE53	0.171206943
RACE55	0.273604446
MV	0.117480441
Apnea	-0.012262741
Infection	0.026450984
GI_other	0.087222647
Depression	0.080231389
Psych_other	0.082623979
Neuropathy	0.069716803
CardioRespShock	0.228794257
Coronary_angina	0.048182744
HD_other	0.015511356
Pneu	0.057607182
Ulcer	0.091465998
Cellulitis	0.095049297
Valvular_Disease	0.078134984
Hypertension_Uncomp	0.087684427
Hypertension_comp	0.143660314
Neurological_Disorders	0.075023091
Diabetes_w_comp	0.077946469
Malnutrition	0.095555424
Morbid_OB	-0.056028398
Endocrine_disorder	0.137464197
Peptic_ulcer	0.114498859
Anemias	0.1663521
Psychosis	0.13049134
Hemiplegia	0.113401107
Heart_failure	0.23205475
Coronary_syndrome	0.110911596
Arrhythmias	0.188301605
Vascular	0.090867219
Renal_failure	0.11154648

### Model Coefficients for Hierarchical Model (COPD)

(Intercept)	-2.170381336
sex2	-0.018743606
AgeAdm	-0.00702047
RACE51	0.29629354
RACE52	0.342336002
RACE53	0.172316947
RACE55	0.275083731
MV	0.112639359
Apnea	-0.017323465
Infection	0.02133693
GI_other	0.095383617
Depression	0.072418589
Psych_other	0.075096553
Neuropathy	0.063679331
CardioRespShock	0.224665848
Coronary_angina	0.056139938
HD_other	0.011352801
Pneu	0.052053617
Ulcer	0.089352719
Cellulitis	0.091640641
Valvular_Disease	0.074608627
Hypertension_Uncomp	0.100372891
Hypertension_comp	0.143513998
Neurological_Disorders	0.070642457
Diabetes_w_comp	0.076044197
Malnutrition	0.089847317
Morbid_OB	-0.045581819
Endocrine_disorder	0.132138897
Peptic_ulcer	0.1109747
Anemias	0.162850779
Psychosis	0.124238457
Hemiplegia	0.109511728
Heart_failure	0.228425309
Coronary_syndrome	0.106258
Arrhythmias	0.19629312
Vascular	0.085350053
Renal_failure	0.106363156
PredCluster2	0.042362651
PredCluster3	0.05007554
PredCluster4	0.052171757

## CMS Models (CMS Standard Model and CMS Hierarchical Model) for COPD

**C-Statistics.** The following table shows C-statistics for the CMS Standard Model and the CMS Hierarchical Model.

	C-Statistic	CI95 (Min)	CI95 (Max)
CMS Standard Model	0.622	0.615	0.629
CMS Hierarchical Model	0.622	0.615	0.629

The following table shows C-statistics for the CMS Standard Model used to predict readmission for patients in each bicluster separately.

	C-Statistic	CI95 (Min)	CI95 (Max)
Bicluster 1	0.587	0.575	0.599
Bicluster 2	0.611	0.598	0.625
Bicluster 3	0.620	0.604	0.636
Bicluster 4	0.638	0.622	0.654

# Model Coefficients for CMS Standard Model (COPD) [14]

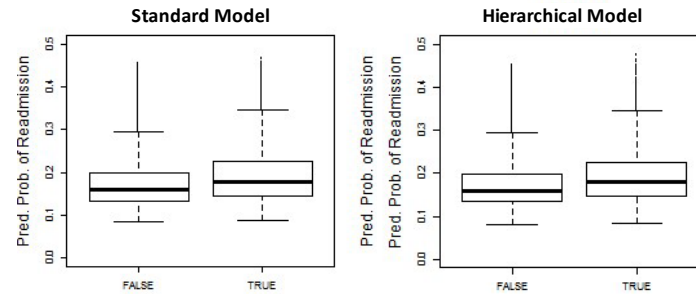
(Intercept)	-2.188594326
V1	-0.004884898
V2	0.173933436
V3	-0.004371274
V4	0.014983286
V5	0.158622714
V6	0.197266795
V7	0.082435098
V8	-0.042473792
V9	0.075588823
V10	0.089748913
V11	-0.042615016
V12	0.146684496
V13	0.381543598
V14	0.085139806
V15	0.075183842
V16	0.114503012
V17	0.16450527
V18	-0.034979967
V19	0.198698509
V20	0.100948646
V21	0.069808662
V22	0.023636931
V23	0.069163157
V24	0.111452974
V25	0.064113847
V26	-0.039814801
V27	0.173239512
V28	0.212336424
V29	0.066160516
V30	0.109441845
V31	0.190317991
V32	0.043561901
V33	0.015612425
V34	0.074089074
V35	0.069126003
V36	0.036551409
V37	0.174960292
V38	0.102815442
V39	0.082962429
V40	0.127491216

### Model Coefficients for CMS Hierarchical Model (COPD)

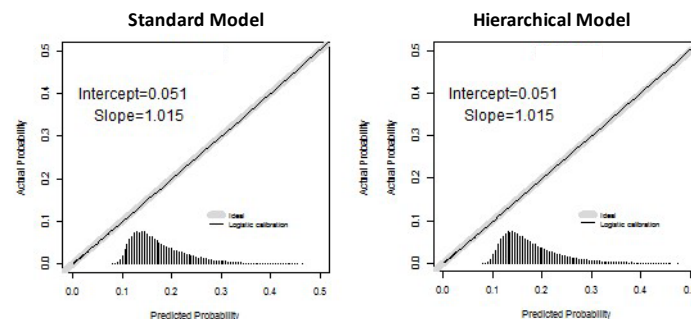
(Intercept)	-2.222560918
V1	-0.005037176
V2	0.164652122
V3	-0.011571161
V4	0.007278066
V5	0.159430966
V6	0.197452639
V7	0.083353046
V8	-0.042706545
V9	0.071953525
V10	0.098535986
V11	-0.030172663
V12	0.143262108
V13	0.382813245
V14	0.081387202
V15	0.086119119
V16	0.11252111
V17	0.150832777
V18	-0.035543286
V19	0.207400734
V20	0.10019542
V21	0.07625943
V22	0.023819484
V23	0.076936963
V24	0.105746192
V25	0.07104448
V26	-0.033998175
V27	0.168407005
V28	0.202506355
V29	0.063304577
V30	0.116819091
V31	0.195860925
V32	0.037067697
V33	0.014270778
V34	0.066636971
V35	0.069127715
V36	0.043952171
V37	0.129843017
V38	0.099065392
V39	0.078360538
V40	0.127042521
PredCluster2	0.098236779
PredCluster3	0.014085719
PredCluster4	0.072649738

## CHF

**Discrimination.** The following are box plots of risk prediction by readmission status for the Standard Model and the Hierarchical Model.



**Calibration.** The following are calibration plots showing logistic regressions relating readmission status to the logistic quantile of the predicted probability of readmission yield regression lines with specified intercept and slope (the ideal regression line would have intercept=0 and slope=1, which is shown shaded for reference). The histograms at the bottom of each graph reflect the frequency of modeled data, horizontal axes show predicted probability, vertical axes show actual probability, and the axes of all figures are constrained to range from 0 to .5.



**Coefficients.** The following are the logistic regression coefficients relating readmission status to the logistic quantile of the predicted probability of readmission for each model, with standard errors.

	Intercept (Standard Error)	Slope (Standard Error)
Standard Model	.009 (0.042)	1.013 (0.027)
Hierarchical Model	0.008 (0.042)	1.013 (0.027)

### Model Coefficients for Standard Model (CHF)

(Intercept)	-1.475389967
sex2	0.074653204
AgeAdm	-0.008514725
RACE51	-0.036053802
RACE52	0.040134152
RACE53	-0.079761067
RACE55	0.072722149
CABG	0.030894001
GI_other	0.056464897
Depression	0.025005144
Psych_other	0.045337378
CardioRespShock	0.048277891
Coronary_angina	0.055087252
HD_other	0.080761149
COPD	0.149282237
Pneu	0.081351108
Dialysis_status	0.173258929
Renal_failure	0.140937411
Nephritis	0.012307007
Other_uri_tract_disorders	0.065712737
Ulcer	0.108579462
Hypertension_Uncomp	0.041031817
Hypertension_Comp	0.105063607
Neuro_Disorders	0.032623414
Hypothyroidism	0.024951326
Obesity	0.026406255
Cancer	0.028160953
Diabetes_w_comp	0.085693489
Malnutrition	0.038386944
Endocrine_disorder	0.093422704
Liver_disease	0.051990801
Peptic_ulcer	0.053199182
Hematological	0.045559899
Anemias	0.123037859
Brain_disorders	-0.00749815
Psychosis	0.093703137
Psychiatric_disorders	0.072868486
Hemiplegia	0.057172104
CHF	0.106985057
Coronary_syndrome	0.096953224
Valvular_disease	0.018311001
Arrhythmia	0.00786506
Stroke	-0.012731604
Vascular	0.061193164

## Model Coefficients for Hierarchical Model (CHF)

(Intercept)	-1.449848979
sex2	0.074706479
AgeAdm	-0.008504158
RACE51	-0.035610416
RACE52	0.04010896
RACE53	-0.079311376
RACE55	0.073284464
CABG	0.024674808
GI_other	0.061045731
Depression	0.029184869
Psych_other	0.049224598
CardioRespShock	0.057426429
Coronary_angina	0.048052865
HD_other	0.089668573
COPD	0.154094768
Pneu	0.089524374
Dialysis_status	0.164539306
Renal_failure	0.139877836
Nephritis	0.004910838
Other_uri_tract_disorders	0.062840363
Ulcer	0.105143831
Hypertension_Uncomp	0.032829812
Hypertension_Comp	0.100497599
Neuro_Disorders	0.040022189
Hypothyroidism	0.029106384
Obesity	0.022538905
Cancer	0.031985591
Diabetes_w_comp	0.082993693
Malnutrition	0.046167614
Endocrine_disorder	0.091753086
Liver_disease	0.060002993
Peptic_ulcer	0.061215338
Hematological	0.054764671
Anemias	0.12180882
Brain_disorders	-0.003163932
Psychosis	0.097984879
Psychiatric_disorders	0.075834723
Hemiplegia	0.065565413
CHF	0.10067029
Coronary_syndrome	0.107487626
Valvular_disease	0.012129124
Arrhythmia	0.001138884
Stroke	-0.003992176
Vascular	0.069322294

PredCluster2	-0.013499297
PredCluster3	-0.039541727
PredCluster4	-0.057008659

## CMS Models (CMS Standard Model and CMS Hierarchical Model) for CHF

**C-Statistics.** The following table shows C-statistics for the CMS Standard Model and the CMS Hierarchical Model.

	C-Statistic	CI95 (Min)	CI95 (Max)
CMS Standard Model	0.602	0.597	0.608
CMS Hierarchical Model	0.602	0.597	0.608

The following table shows C-statistics for the CMS Standard Model used to predict readmission for patients in each bicluster separately.

	C-Statistic	CI95 (Min)	CI95 (Max)
Bicluster 1	0.573	0.563	0.583
Bicluster 2	0.590	0.579	0.600
Bicluster 3	0.603	0.591	0.614
Bicluster 4	0.614	0.603	0.626

# Model Coefficients for CMS Standard Model (CHF) [15]

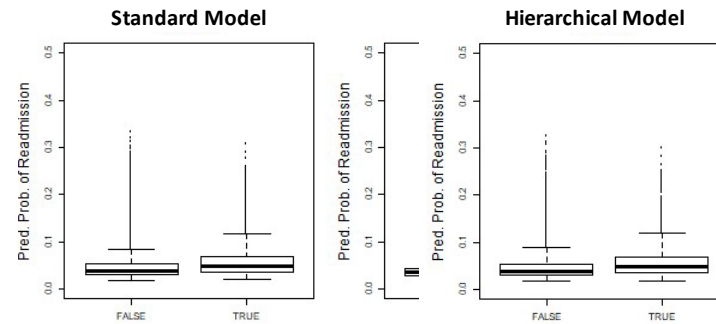
(Intercept)	-2.062052423
V1	-0.008807384
V2	0.08069205
V3	0.026511089
V4	0.059292935
V5	0.021486724
V6	0.083551993
V7	0.043335937
V8	0.110433094
V9	0.050644153
V10	0.055051891
V11	0.063148831
V12	0.046434593
V13	0.130099365
V14	-0.001401658
V15	0.096204102
V16	0.074628886
V17	0.02554376
V18	0.045885408
V19	0.072014832
V20	0.053421316
V21	0.124207717
V22	0.105487347
V23	0.051450424
V24	0.021372813
V25	0.01075549
V26	0.086498498
V27	-0.001335018
V28	0.070577466
V29	0.142129454
V30	0.046599464
V31	0.042236327
V32	0.07795193
V33	0.206227519
V34	0.170726009
V35	0.05424802
V36	0.071097061
V37	0.117969103

### Model Coefficients for CMS Hierarchical Model (CHF)

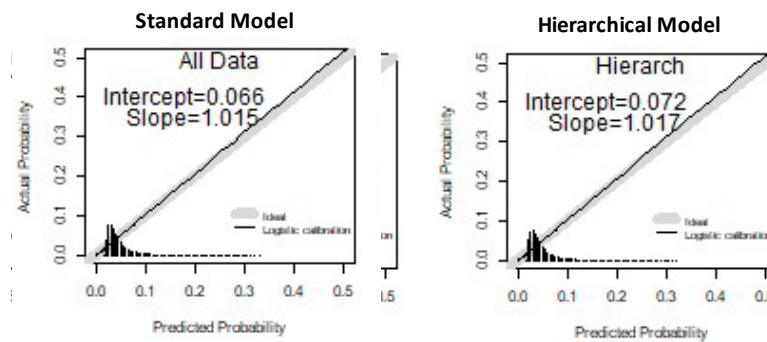
(Intercept)	-2.050961429
V1	-0.008696382
V2	0.080417206
V3	0.024568048
V4	0.060401182
V5	0.026470131
V6	0.07824069
V7	0.055357171
V8	0.100353589
V9	0.061970384
V10	0.066594667
V11	0.068254076
V12	0.058624423
V13	0.120852698
V14	0.005596376
V15	0.102047312
V16	0.079661612
V17	0.031011406
V18	0.050815364
V19	0.084441452
V20	0.065024208
V21	0.119511648
V22	0.11654221
V23	0.047832743
V24	0.0189412
V25	0.007449149
V26	0.097154811
V27	0.009679744
V28	0.079037213
V29	0.147713008
V30	0.04662239
V31	0.041108317
V32	0.088384596
V33	0.190553921
V34	0.160246633
V35	0.035498901
V36	0.061096207
V37	0.106604226
PredCluster2	0.028721208
PredCluster3	-0.029432347
PredCluster4	-0.048839832

## TKA/THA

**Discrimination.** The following are box plots of risk prediction by readmission status for the Standard Model and the Hierarchical Model.



**Calibration.** The following are calibration plots showing logistic regressions relating readmission status to the logistic quantile of the predicted probability of readmission yield regression lines with specified intercept and slope (the ideal regression line would have intercept=0 and slope=1, which is shown shaded for reference). The histograms at the bottom of each graph reflect the frequency of modeled data, horizontal axes show predicted probability, vertical axes show actual probability, and the axes of all figures are constrained to range from 0 to .5.



**Coefficients.** The following are logistic regression coefficients relating readmission status to the logistic quantile of the predicted probability of readmission for each model, with standard errors.

	Intercept (Standard Error)	Slope (Standard Error)
Standard Model	0.066 (0.092)	1.015 (0.031)
Hierarchical Model	0.072 (0.092)	1.017 (0.031)

### Model Coefficients for Standard Model (TKA/THA)

(Intercept)	-6.263520554
sex2	-0.156977542
AgeAdm	0.037561114
RACE51	0.107946335
RACE52	0.385560747
RACE53	0.083620721
RACE55	0.103221123
Renal_failure	0.367756519
Major_Symp_Abnormalities	0.173001919
Hypertension_Uncomp	0.115321908
Hypertension_Comp	0.034487102
Morbid_OB	0.1284828
Endocrine_disorders	0.221828594
Psychiatric_disorders	0.321401406
CHF	0.21488135
Coronary_angina	0.263264479
Arrhythmia	0.24838679
COPD	0.389660791

# Model Coefficients for Hierarchical Model (TKA/THA)

(Intercept)	-6.257678633
sex2	-0.156625896
AgeAdm	0.037256943
RACE51	0.104795822
RACE52	0.38085003
RACE53	0.080648574
RACE55	0.100025632
Renal_failure	0.326415209
Major_Symp_Abnormalities	0.143870143
Hypertension_Uncomp	0.109878666
Hypertension_Comp	0.028345431
Morbid_OB	0.068228389
Endocrine_disorders	0.209295683
Psychiatric_disorders	0.439980871
CHF	0.241863504
Coronary_angina	0.242997744
Arrhythmia	0.236970594
COPD	0.294032113
PredCluster2	0.101832731
PredCluster3	0.060642002
PredCluster4	0.117407922
PredCluster5	0.201783265
PredCluster6	0.14290807
PredCluster7	-0.0369165

## CMS Models (CMS Standard Model and CMS Hierarchical Model) for TKA/THA

**C-Statistics.** The following table shows C-statistics for the CMS Standard Model and the CMS Hierarchical Model.

	C-Statistic	CI95 (Min)	CI95 (Max)
<b>CMS Standard Model</b>	0.648	0.640	0.657
<b>CMS Hierarchical Model</b>	0.648	0.640	0.657

The following table shows C-statistics for the CMS Standard Model used to predict readmission for patients in each bicluster separately.

	C-Statistic	CI95 (Min)	CI95 (Max)
<b>Bicluster 1</b>	0.585	0.561	0.609
<b>Bicluster 2</b>	0.632	0.609	0.655
<b>Bicluster 3</b>	0.617	0.594	0.641
<b>Bicluster 4</b>	0.630	0.606	0.653
<b>Bicluster 5</b>	0.608	0.583	0.632
<b>Bicluster 6</b>	0.589	0.562	0.615
<b>Bicluster 7</b>	0.640	0.621	0.659

# **Model Coefficients for CMS Standard Model (TKA/THA) [16]**

(Intercept)	-4.007625537
Var1	0.036039292
Var2	-0.149437339
Var3	0.088157516
Var4	0.252326647
Var5	-0.255229777
Var6	0.234030925
Var7	0.131248955
Var8	0.118415513
Var9	-0.014234681
Var10	0.158442117
Var11	0.186149829
Var12	0.10822119
Var13	0.120553114
Var14	0.213179137
Var15	0.166404922
Var16	0.244882944
Var17	0.260963406
Var18	0.228775313
Var19	0.099773803
Var20	0.167375189
Var21	0.236389437
Var22	0.08572084
Var23	0.22805813
Var24	0.092669018
Var25	0.099767352
Var26	0.363700358
Var27	0.038962561
Var28	0.582409201
Var29	0.317306501
Var30	0.103490531
Var31	-0.001329201
Var32	0.026795269
Var33	0.150796704

### Model Coefficients for CMS Hierarchical Model (TKA/THA)

(Intercept)	-4.0316433
Var1	0.035679265
Var2	-0.148849333
Var3	0.08807725
Var4	0.25290998
Var5	-0.257380043
Var6	0.241117802
Var7	0.132427427
Var8	0.115796146
Var9	-0.014769398
Var10	0.15814836
Var11	0.187159646
Var12	0.035368612
Var13	0.120886777
Var14	0.211303719
Var15	0.170049309
Var16	0.245655958
Var17	0.387470462
Var18	0.234387939
Var19	0.102192659
Var20	0.187162267
Var21	0.20830413
Var22	0.084196245
Var23	0.206829049
Var24	0.096990789
Var25	0.103278456
Var26	0.256166878
Var27	0.069134573
Var28	0.601609967
Var29	0.294460582
Var30	0.109616297
Var31	0.003492241
Var32	0.030762491
Var33	0.117221489
PredCluster2	0.132189893
PredCluster3	0.074260901
PredCluster4	0.096335076
PredCluster5	0.225685704
PredCluster6	0.166772439
PredCluster7	-0.034196246

## REFERENCES

1. SAS. Using SAS® to Perform Individual Matching in Design of Case-Control Studies 2010 [cited 2020 May, 5th]. Available from: <https://support.sas.com/resources/papers/proceedings10/061-2010.pdf>.
2. Islam MM, Valderas JM, Yen L, Dawda P, Jowsey T, McRae IS. Multimorbidity and comorbidity of chronic diseases among the senior Australians: prevalence and patterns. PloS one. 2014;9(1):e83783. Epub 2014/01/15. doi: 10.1371/journal.pone.0083783. PubMed PMID: 24421905; PubMed Central PMCID: PMC3885451.
3. Newman MEJ. Networks: An Introduction. Oxford, United Kingdom: Oxford University Press; 2010.
4. Treviño S, Nyberg A, Del Genio CI, Bassler KE. Fast and accurate determination of modularity and its effect size. Journal of Statistical Mechanics: Theory and Experiment. 2015;2015(2):P02003. doi: 10.1088/1742-5468/2015/02/p02003.
5. Chauhan R, Ravi J, Datta P, Chen T, Schnappinger D, Bassler KE, et al. Reconstruction and topological characterization of the sigma factor regulatory network of Mycobacterium tuberculosis. Nature communications. 2016;7:11062. Epub 2016/04/01. doi: 10.1038/ncomms11062. PubMed PMID: 27029515; PubMed Central PMCID: PMC4821874.
6. Bhavnani SK, Dang B, Penton R, Visweswaran S, Bassler KE, Chen T, et al. How High-Risk Comorbidities Co-Occur in Readmitted Patients With Hip Fracture: Big Data Visual Analytical Approach. JMIR Med Inform. 2020;8(10):e13567. doi: 10.2196/13567.
7. Rand WM. Objective Criteria for the Evaluation of Clustering Methods. Journal of the American Statistical Association. 1971;66(336):846-50. doi: 10.2307/2284239.
8. Fruchterman T, Reingold E. Graph Drawing by Force-Directed Placement. Software – Practice & Experience. 1991;21(11):1129–64.
9. Dang B, Chen T, Bassler KE, Bhavnani SK. ExplodeLayout: Enhancing the Comprehension of Large and Dense Networks. AMIA Jt Summits Transl Sci Proc 2016.
10. Bhavnani SK, Chen T, Ayyaswamy A, Visweswaran S, Bellala G, Rohit D, et al. Enabling Comprehension of Patient Subgroups and Characteristics in Large Bipartite Networks: Implications for Precision Medicine. Proceedings of AMIA Joint Summits on Translational Science. 2017:21-9. Epub 2017/08/18. PubMed PMID: 28815099; PubMed Central PMCID: PMC5543384.
11. Hastie T, Tibshirani R, Friedman J. The Elements of Statistical Learning. New York, NY, USA: Springer New York Inc.; 2001.
12. Medicare Payment Advisory Commission (MedPAC). Report to the Congress: Medicare and the Health Care Delivery System. Chapter 3. Approaches to Bundle Payment for Post-Acute Care Washington, DC2013 [updated June]. 57-88]. Available from: [http://www.medpac.gov/documents/reports/jun13\\_ch03.pdf?sfvrsn=0](http://www.medpac.gov/documents/reports/jun13_ch03.pdf?sfvrsn=0).

13. Evaluation YNHHSccFOR. Procedure-Specific Measures Updates and Specifications Report Hospital-Level 30-Day Risk-Standardized Readmission Measures. A report prepared for the Centers for Medicare & Medicaid Services (CMS) 2017 [June 1, 2017]. Available from: <https://www.cms.gov/Medicare/Quality-Initiatives-Patient-Assessment-Instruments/HospitalQualityInits/Measure-Methodology.html>.
14. Yale New Haven Health Services Corporation/Center for Outcomes Research & Evaluation. 2015 Condition-specific measures updates and specifications report: Hospital-level 30-day risk-standardized readmission measures on acute myocardial infarction, heart failure, pneumonia, chronic obstructive pulmonary disease, and stroke. A report prepared for the Centers for Medicare & Medicaid Services (CMS) 2015 [April 20, 2015]. Available from: <http://www.cms.gov/Medicare/Quality-Initiatives-Patient-Assessment-Instruments/HospitalQualityInits/Measure-Methodology.html>.
15. Keenan PS, Normand SL, Lin Z, Drye EE, Bhat KR, Ross JS, et al. An administrative claims measure suitable for profiling hospital performance on the basis of 30-day all-cause readmission rates among patients with heart failure. *Circ Cardiovasc Qual Outcomes*. 2008;1(1):29-37. Epub 2008/09/01. doi: 10.1161/circoutcomes.108.802686. PubMed PMID: 20031785.
16. Yale New Haven Health Services Corporation/Center for Outcomes Research & Evaluation. 2015 Procedure-specific readmission measures updates and specifications report: Elective primary total hip arthroplasty and/or total knee arthroplasty, and isolated coronary artery bypass graft surgery. A report prepared for the Centers for Medicare & Medicaid Services (CMS) 2015 [April 20, 2015]. Available from: <http://www.cms.gov/Medicare/Quality-Initiatives-Patient-Assessment-Instruments/HospitalQualityInits/Measure-Methodology.html>.